Sex difference in tDCS current mediated by changes in cortical anatomy: a study across young, middle and older adults

Bhattacharjee, Sagarika; Kashyap, Rajan; Goodwill, Alicia M.; O'Brien, Beth Ann; Rapp, Brenda; Oishi, Kenichi; Desmond, John E.; Chen, Annabel Shen-Hsing

2022

Bhattacharjee, S., Kashyap, R., Goodwill, A. M., O'Brien, B. A., Rapp, B., Oishi, K., Desmond, J. E. & Chen, A. S. (2022). Sex difference in tDCS current mediated by changes in cortical anatomy: a study across young, middle and older adults. Brain Stimulation, 15(1), 125-140. https://dx.doi.org/10.1016/j.brs.2021.11.018

https://hdl.handle.net/10356/163239

https://doi.org/10.1016/j.brs.2021.11.018

Brain Stimulation 15 (2022) 125–140

Contents lists available at ScienceDirect

Brain Stimulation

journal homepage: http://www.journals.elsevier.com/brain-stimulation

Sex difference in tDCS current mediated by changes in cortical anatomy: A study across young, middle and older adults

Sagarika Bhattacharjee, M.B.B.S, M.D, PhD [a, *], Rajan Kashyap, PhD [b], Alicia M. Goodwill, PhD [b, c], Beth Ann O'Brien, PhD [d], Brenda Rapp, PhD [e], Kenichi Oishi, M.D, PhD [f], John E. Desmond, PhD [f, 1], S.H. Annabel Chen, PhD [a, b, g, **]

[a] Psychology, School of Social Sciences, Nanyang Technological University, Singapore
[b] Centre for Research and Development in Learning (CRADLE), Nanyang Technological University, Singapore
[c] Physical Education and Sports Science Academic Group, National Institute of Education, Nanyang Technological University, Singapore
[d] Centre for Research in Child Development (CRCD), National Institute of Education, Singapore
[e] The Johns Hopkins University, Krieger School of Arts and Sciences, Baltimore, United States
[f] The Johns Hopkins University School of Medicine, Baltimore, United States
[g] Lee Kong Chian School of Medicine (LKC Medicine), Nanyang Technological University, Singapore

ARTICLE INFO

Article history:
Received 19 June 2021
Received in revised form
11 November 2021
Accepted 22 November 2021
Available online 23 November 2021

Keywords:
tDCS current
Torque
Cortical volume
Simulated current

ABSTRACT

Introduction: The observed variability in the effects of transcranial direct current stimulation (tDCS) is influenced by the amount of current reaching the targeted region-of-interest (ROI). Age and sex might affect current density at target ROI due to their impact on cortical anatomy. The present tDCS simulation study investigates the effects of cortical anatomical parameters (volumes, dimension, and torque) on simulated tDCS current density in healthy young, middle-aged, and older males and females.

Methodology: Individualized head models from 240 subjects (120 males, 18–87 years of age) were used to identify the estimated current density (2 mA current intensity, 25 cm^2 electrode) from two simulated tDCS montages (CP5_CZ and F3_FP2) targeting the inferior parietal lobule (IPL) and middle frontal gyrus (MFG), respectively. Cortical parameters including segmented brain volumes (cerebrospinal fluid [CSF], grey and white matter), cerebral-dimensions (length/width & length/height) and brain-torque (front and back shift, petalia, and bending) were measured using the magnetic resonance images (MRIs) from each subject. The present study estimated sex differences in current density at these target ROIs mediated by these cortical parameters within each age group.

Results: For both tDCS montages, females in the older age group received higher current density than their male counterparts at the target ROIs. No sex differences were observed in the middle-aged group. Males in the younger age group had a higher current density than females, only for the parietal montage. Across all age groups, CSF, and grey matter volumes significantly predicted the current intensity estimated at the target sites. In the older age group only, brain-torque was a significant mediator of the sex difference.

Conclusions: Our findings demonstrate the presence of sex differences in the simulated tDCS current density, however this pattern differed across age groups and stimulation locations. Future studies should consider influence of age and sex on individual cortical anatomy and tailor tDCS stimulation parameters accordingly.

Abbreviations: tDCS, transcranial direct current stimulation; ROI, region of interest; w-target, current density at target region; GM, Grey matter volume; WM, White matter volume; CSF, cerebrospinal fluid volume; IPL, Inferior parietal lobule; MFG, Middle Frontal Gyrus.

* Corresponding author. School of Social Sciences, College of Humanities, Arts, & Social Sciences, 48 Nanyang Ave, 639818, Singapore.
** Corresponding author. School of Social Sciences, College of Humanities, Arts, & Social Sciences, 48 Nanyang Ave, 639818, Singapore.
E-mail addresses: bhattacharya.sagarika7@gmail.com, SAGARIKA001@e.ntu.edu.sg (S. Bhattacharjee), rajankashyap6@gmail.com (R. Kashyap), alicia.goodwill@nie.edu.sg (A.M. Goodwill), obrienbeth1@gmail.com (B.A. O'Brien), brapp1@jhu.edu (B. Rapp), koishi@mri.jhu.edu (K. Oishi), jdesmon2@jhmi.edu (J.E. Desmond), annabelchen@ntu.edu.sg (S.H.A. Chen).
[1] Senior Author.

https://doi.org/10.1016/j.brs.2021.11.018

1. Introduction

Non-invasive brain stimulation, such as transcranial direct current stimulation (tDCS), has received increased interest in the last 20 years [1]. In tDCS, two or more electrodes are positioned (referred to as a 'montage') over the scalp, and a low-intensity current is passed through the cortex [1]. tDCS can modulate behavior by stimulating the underlying target region of interest (ROI) in the brain. Application of low-level electrical current at the subthreshold level modulates the resting membrane potential of the underlying neurons and alters the threshold at which the neuron generates action potentials [2]. tDCS effects are generally polarity dependent where anodal stimulation excites and cathodal stimulation inhibits the underlying membrane potential [3]. However, the effects of tDCS are likely to be complex as great inter-individual variability is seen in tDCS induced outcomes [4–7], such as neurophysiological (motor evoked potential [MEP] changes) [8,9], behavioural (e.g., working memory performance) [10], and neurotransmitter (e.g., GABA or glutamate) concentration [11] measures. Understanding the underlying mechanism of such variability is essential to determine precision in designing stimulation protocol for optimal behavioural outcomes and clinical application.

One factor thought to contribute to the tDCS-induced response variability is the simulated electric field strengths at the target ROI [8,9,11,12], which could indirectly vary with the individual differences in neuroanatomy features [13]. Recently, Mosayebi-Samani et al. [13] reported that individual anatomical factors like regional cerebrospinal fluid (CSF) thickness and the electrode to cortex distance could directly correlate with tDCS-induced neurophysiological effects. This highlights the importance of investigating inter-individual variations in cortical anatomy with the simulated current density at a given target ROI. Such an investigation is expected to have implications in future tDCS studies. This is because controlling the total current density received at a target ROI is vital for optimizing the stimulation effect across participants. tDCS currents are simulated using a finite element modelling approach where each participant's T1-weighted magnetic resonance images (MRIs) are converted into a head model [14]. The simulated electric field measures correlate with in-vivo recorded electrical field following tDCS [15] and thus are widely accepted as an indirect estimation of the electric current distribution in the brain following tDCS.

Prior research studies suggest that simulated current density at a target ROI decreases with increasing age [9,16,17]. The increase in cerebrospinal fluid volume that is often associated with age-related brain atrophy [9] could be a potential factor for such a decrease in current density. It is important to highlight that most of these tDCS studies were performed on small cohorts of individuals (number of images = 10 approximately) and that large sample sizes can be beneficial for generalizing our understanding across the population. Indahlastari et al. [16] simulated two montages (F3–F4 and M1-SO) on a large cohort of 587 healthy adults (mean age = 73.9 years, range = 51–95 years) and found that current density at the target ROIs (dorsolateral prefrontal cortex and precentral gyrus) decreases with increasing age. They used mediation analysis and reported that a decrease in the global brain-to-CSF ratio mediates the association between age and current intensity at a target ROI. However, their study was limited to older adults only. It is undeniable that the brain morphometry changes over the lifespan and investigation of its impact on simulated current density would be beneficial. On this ground, a recent study compared 20 younger (20–35 years) and 20 older (64–79 years) individuals. They revealed that the prominent inverse relationship of tissue volumes (skin, skull and CSF) with electric field strengths seen in young age gets mitigated in the older age group [11]. Therefore, it could be informative to evaluate differences in the current intensity at a target ROI across various age groups comprising a large cohort of young, middle, and older individuals.

There has been considerable research evaluating the impact of the aging brain and current intensity at targeted ROIs, but their association with sex has been neglected so far [18]. Such investigation becomes especially important when many empirical studies are exclusively reporting sex to be an important variable determining the tDCS outcomes (summarized in Table 1). As noted in Table 1, there is inconsistency regarding the effectiveness of tDCS across the sexes (males or females), thereby increasing the need to investigate sex difference in tDCS. Moreover, these studies were primarily conducted in a younger cohort, lacking information about sex differences in tDCS outcome across different age groups. In this aspect, a meta-analysis on 61 studies [19] with participants ranging from 19 to 79 years revealed that the tDCS effects are strongly influenced by the percentage of females in the cohort. In an attempt to investigate the cumulative effect of age and sex, one study [20] combined the data from two separate experiments conducted on young (mean age 23 years) [21] and healthy adults (mean age 67.9 years) [22]. They showed that older females performed better following tDCS stimulation, whereas young females did not show any difference in performance compared to their respective control groups. Their findings suggest males and females may respond to tDCS differently at different ages. To support the sex difference in tDCS outcomes, only one simulation study with MRI images of 5 males and 5 females (spanning ages 27–47 years) reported females having higher current density at the motor cortex than males [23]. They attributed this difference to anatomical differences in grey matter (GM), white matter (WM), and CSF volumes [23]. It is evident that there is a lack of investigations about the cumulative effect of age and sex on the current intensity at target ROI while considering the anatomical factors that differ between males and females.

It is known that age-related changes in the anatomy of the cortex differ between males and females, and sex plays a vital role in various neuroscientific findings [24]. For example, the sex differences in various cortical macro-anatomic features such as brain volumes, size, and left-right cortical asymmetry have been well documented [refer to review, 15]. The most consistent finding is the larger brain volume for men accounted for by a larger body dimension than females [25–29]. However, if variations in brain size are adjusted, inconsistent findings are reported. For example, some studies reported a higher percentage of GM in females [29,30], or a larger GM [28] and WM proportions in males [29,31–33], while some studies did not report any sex differences [34,35]. In this aspect, studies have indicated that brain size (rather than sex) is the primary variable, as no differences in the GM volume proportions were detected when brain-size matched male and female brains were compared [25,30]. Age-related global GM atrophy was also reported to be higher in women (−4.7 cm3/year, −0.91%/year) than men (−3.3 cm3/year, −0.65%/year) in a longitudinal study conducted over 1172 healthy older adults (age >65 years) [36]. Many studies also investigated possible sex differences in brain asymmetry when the anatomy of left and right hemispheres were compared. Such asymmetry is not well understood but is often associated with the left-right handedness or the hemispheric specialization of functions [37]. In this aspect, one of the significant structural asymmetries is known as Yakovlevian torque (Fig. 1). It refers to an anticlockwise twist of the brain around the ventral-dorsal axis [37,38]. This shape asymmetry is proposed to be unique to humans, and the specific right-frontal and left-occipital protrusion is present in 60% of the human population [37]. It consists of three components (see Fig. 1A): (a) "Shift" is the displacement of the left hemisphere with the right hemisphere in the dorsal-ventral direction, (b) "Petalia" is a posterior shift of the

Table 1
Studies that have reported a sex difference in the outcomes of tDCS stimulation (N = number of participants, M = Male, F = Female).

Paper	N	Age group	Outcome measures under investigation	Electrode size	Electrode position	Target region	Current	Duration
Behavioural tasks as an outcome measure following tDCS								
Females showing better performance than men following tDCS								
Younger age group								
Adenzato et al., 2017 [21]	16 M, 16 F	F = 24.2 ± 3.7 M = 23.0 ± 3.2	Theory of Mind	7 × 5 cm^2	Anode = Fp2 Cathode = Pz	mPFCS	1 mA	6 min
Females showed a significant decrease in reaction time post-stimulation, whereas males did not.								
Gallucci et al., 2020 [45]	45 M, 45F	22.2 ± 2.46	Aggression	5 × 5 cm^2 anode, 7 × 5 cm^2 cathode	Anode = F6 Cathode = F5	Right and Left VLPFC	1.5 mA	20 min
Females show a significant increase in aggression rating following stimulation.								
Yang et al., 2018 [46]	27 M, 25F	F = 21.44 ± 1.88 M = 22.30 ± 2.21	Search behaviour	5 × 7 cm^2	Anode = F3 Cathode = F4	DLPFC area	2 mA	20min
Female subjects significantly increased their accepted point right anodal/left cathodal stimulation, but the change was not significant in males								
Fumagalli et al., 2010 [47]	38 M, 40F	F = 23.7 ± 0.57, M = 25.7 ± 1.03	Moral Judgement task	Anode = 54 cm^2; Cathode = 64 cm^2	*Condition 1* Anode = forehead *Condition 2* Anode = Occipital cortex Cathode = deltoid in both the conditions	Ventral PFC, or Occipital Cortex	2 mA	15min
Females had a significant change in task reaction time post tDCS on ventral PFC compared to tDCS on the occipital cortex.								
Boggio et al., 2008 [48]	7 M, 7F	23.4 ± 6.8	Go-no Go task	5 × 7cm2	Anode = T3 Cathode = T4	Superior Temporal Sulcus	2 mA	8min
Independent of stimulation condition, women had significantly more correct answers when compared to men. Women made significantly fewer errors following active tDCS compared to sham stimulation. Men made significantly more errors during active stimulation compared to sham								
Gao et al., 2018 [49]	44 M, 46F	Not provided	Deception task	5 × 7 cm2	Anode = F3 Cathode = F4	DLPFC	2 mA	20min
Right anodal and left cathodal activity on DLPFC only significantly decreased female subjects' deception.								
Ye et al., 2015 [50]	24 M, 36F	21.3	Working memory	5 × 7 cm^2	Anode = F4 Cathode = F3	DLPFC	2 mA	15 min
Females demonstrated a significant difference in working memory compared to sham. The male group displayed the same tendency but was not significant.								
León et al., 2020 [51]	41 M, 50F	F = 22.28 ± 6.44 M = 21.02 ± 5.29	Real-world decision-making processes	Anode = 9 cm^2 Cathode = 25 cm^2	Anode = Fp2 Cathode = contralateral trapezius	Orbito frontal area	1.5 mA	20 min
Anodal tDCS increased the task performance in women compared to sham, but a similar stimulation effect is not seen in males.								
Lapenta et al., 2012 [52]	14 M, 14F	23.2 ± 3.1	Multisensory task integrating shapes and non-words	5 × 7 cm^2	Anode = between T3 and T4 Cathode = right arm	Temporal cortex	1 mA	15 min
The performance in men was poorer than women on the no-go condition for congruent stimuli during cathodal tDCS.								
Martin et al., 2017 [53]	20 M, 20F	F = 21.6 ± 2.7/M = 24.1 ± 5.5	Theory of mind task through reading the mind in eye test (RMET)	4 × 1 HD-tDCS	Anode = locating 15% of the distance from the Fz toward the FPz	dmPFC	1 mA	20 min
Anodal stimulation to the dmPFC increased accuracy on the RMET task compared to sham only in females.								
Workman et al., 2020 [54]	10 M, 10 F	Mean age 24.6 ± 3.8	Isokinetic fatigue testing	5 × 7 cm^2	Anode = C3 Cathode = Contralateral SO	M1	2 mA and 4 mA	20 min
Females had significantly greater knee extensor fatigability at only 4 mA *compared to men*								
Middle or Older age group								
Frank et al., 2012 [55]	32 tinnitus patients 25 M,7F	54.2 ± 10.0	Tinnitus scores	Not provided	Anode = F3 Cathode = F4	DLPFC area	1.5 mA	30 min on 2 days per week for 3-weeks
Female patients showed superior treatment response in contrast to male patients								
Adenzato et al., 2019 [22]	15 M and 15F per anodal and cathodal group	67.9 ± 6.1	Theory of mind	7 × 5 cm^2	Anode = Fp2 Cathode = between Oz and inion	mPFC	1.5 mA	6 min
Female participants were slower to decide after anodal tDCS than a sham, whereas males did not show any effect.								
Males showing better performance than females following tDCS								
Younger age group								
Bertossi et al., 2017 [56]	24 M, 24F	F = 23.3 M = 23.0	Daydreaming, Working memory	5 × 5 cm^2 cathode, 7 × 5 cm^2 anode	Anode = Fpz Cathode = deltoid	mPFC	2 mA	15 min
Males show a significant reduction in the mean scores compared to sham, whereas females did not show a significant change								
Wang et al., 2019 [57]	96 M, 96F	F = 20.2 ± 1.5 M = 20.5 ± 2	Decision making task	5 × 7 cm^2	Anode = FPz Cathode = Oz	mPFC	1.5 mA	20 min
Males showed a significant decrease in implicit association test scores following stimulation, whereas females did not show any significant change post-stimulation compared to sham.								
	10 M, 10F			35 cm^2			2 mA	20 min

(continued on next page)

Table 1 (*continued*)

Paper	N	Age group	Outcome measures under investigation	Electrode size	Electrode position	Target region	Current	Duration
Tommaso et al., 2014 [58]		F = 25.5 + 4.3 M = 25.3 + 3.8	Bisection line and computer supported attention task		Anode = P3 Cathode = Supraorbital cortex	Left parietal Cortex		
Males showed reduced error than females following tDCS, whereas oestrogen fluctuations could influence the bisection-line test in females during the menses, follicular and luteal phases.								
Fehring et al., 2021 [59]	37 females, 36 males	18–32 years old	Practice-related learning in the Stop-Signal Task	Anode = 2.5 × 4 cm Cathode = 4 × 6 cm	Anode = F3 Cathode = Right supraorbital area	DLPFC	1.5 mA	10 min
The effects of tDCS on response execution (percentage of correct responses) were higher for males but lower for females								
Bhattacharjee et al., 2019, 2020 [60,61]	8 M, 6 F	F = M =	Reading task	5 × 5 cm^2	Anode = CP5 Anode = TP7 Cathode = Cz	Left IPL and left MTG	2 mA	20 min
Males showed better improvement in reading performance post-stimulation for both the montages								
Neurophysiological parameters as outcome measures of tDCS								
Kuo et al., 2006 [62]	52 M,66F	F = 26.2 ± 2.2 M = 27.4 ± 3.9	Motor cortex excitability (MEPs)	5 × 7 cm^2	Anode = representational area of the right abductor digiti minimi muscle (ADM) as determined by transcranial magnetic stimulation (TMS), Cathode = the right orbit.		2 mA for (1)4s (intra direct current effect) (2)19min (cathodal) (3)13 min (anodal)	
The excitability-diminishing after-effects of cathodal tDCS were prolonged in females compared to males. Similarly, the female group showed more inhibition than males during a short tDCS that elicits no after-effects. In contrast, excitability-enhancing anodal tDCS resulted in no significant differences between the sexes.								
Chaieb et al., 2008 [63]	22 M, 24F	F = 23.6 ± 2.4 M = 27.2 ± 5.4	Visual Evoked Potential	5 × 7 cm^2	Anode = Oz Cathode = Cz	Visual cortex	1 mA	10 min
Females showed significantly higher cortical excitability following anodal stimulation compared to the age-matched males.								
Lee et al., 2018 [64]	15 M, 14 F	F = 22.92 ± 3.25 M = 23.33 ± 4.56	TMS-EEG to elicit and record TMS-evoked potentials (TEPs)	35 cm2	Anode = F3 Cathode = Contralateral orbit	DLPFC	1 mA	15 min
That study found that tDCS targeting the DLPFC resulted in higher motor excitability in females during high estrogen state compared to women with low oestrogen state and males								

left hemisphere relative to the right hemisphere in the anterior-posterior direction, (c) "Bending" corresponds to the angle at which the cortical tissue in one hemisphere crosses the midline to displace the tissue in another hemisphere. Studies have found that variability in structural asymmetry is associated with both sex and age [39]. For example, one study reported that right frontal petalia (in right-handers and left-handers) and occipital petalia (in left-handers only) are strongly lateralized in men compared to women [40]. These findings were in accordance with the prior findings of greater frontal and occipital asymmetries in men which is reversed in women [41]. Progressive decrease in degree of asymmetry is also seen with age related cerebral atrophy [42]. Owing to such age related changes in cortical anatomy between men and women, it is expected that the total current intensity at target ROI might also differ.

These sex differences in cortical anatomy motivated the present study to investigate its contribution to simulated current density at target ROI and how it varies across young, middle, and older age groups. Thus, the present study simulated tDCS electric field on a large sample (n = 240) of individual MRIs using an individualized approach. Two montages CP5_CZ and F3_FP2 were simulated targeting two ROIs left inferior parietal lobule (IPL) and left middle frontal gyrus (MFG), respectively. These two montages were selected because most of the tDCS studies uses these two montages to modulate specific cognitive functions such as reading behaviour (CP5_CZ) [43] and depression (F3_FP2) [44]. At the same time, simulating these two montages can reveal the differences created by two different stimulation locations (parietal and frontal regions) in tDCS current. Fifteen anatomical parameters that could influence tDCS current distribution, including cerebral-volume, -dimension, and -torque measures, were extracted to characterize each brain. Finally, the association between demographic factors (age and sex), anatomical factors (volume, dimension, and torque), and current intensity at target ROI were analyzed.

2. Methodology

The study investigated the influence of demographics (age and sex), volume and dimension of underlying anatomical tissue types, and brain asymmetry on tDCS current density at target ROI. The tDCS current was simulated on 240 individual MRIs of males and females across three age groups (young, middle, and older adults) using Realistic Volumetric-Approach-Based Simulator (ROAST) [65]. Each T1 image was simulated for two standard montages CP5_CZ and F3_Fp2. ROAST outputs from each brain were post-processed to estimate current density at the two targets ROIs: left IPL and left MFG using a toolbox Individual-Systematic Approach for tDCS Analysis (i-SATA) developed in our previous work [66]. The morphometric parameters (i) brain volumes (CSF, GM, and WM), (ii) dimensions (length, breadth, and height), and (iii) torque (petalia, shift, and bending) were estimated from each MRI. Finally, four statistical analyses (details in section 2.3) were performed to investigate the effect of age and sex on the current density at target ROI and evaluate the contribution of underlying cortical anatomy.

2.1. Data description

We obtained the T1 weighted MRI images from the repository of the Cambridge Centre for Ageing and Neuroscience (Cam-CAN) study cohort stage 2 (for details, please refer to Taylor et al. and Shafto et al. [67,68]). The repository contains multimodal (MRI and cognitive-behavioral) cross-sectional data from a population-based sample of a large cohort (approximately N = 700) across the adult lifespan (18–87 years old). The data was collected in three stages, and all participants were asked to provide written consent before recruitment into the first stage. Stage 1 consisted of a home-based interview of 2681 participants with demographic information, measures of health (cognitive, mental, and physical), and lifestyle information. Those cognitively normal participants who [MMSE

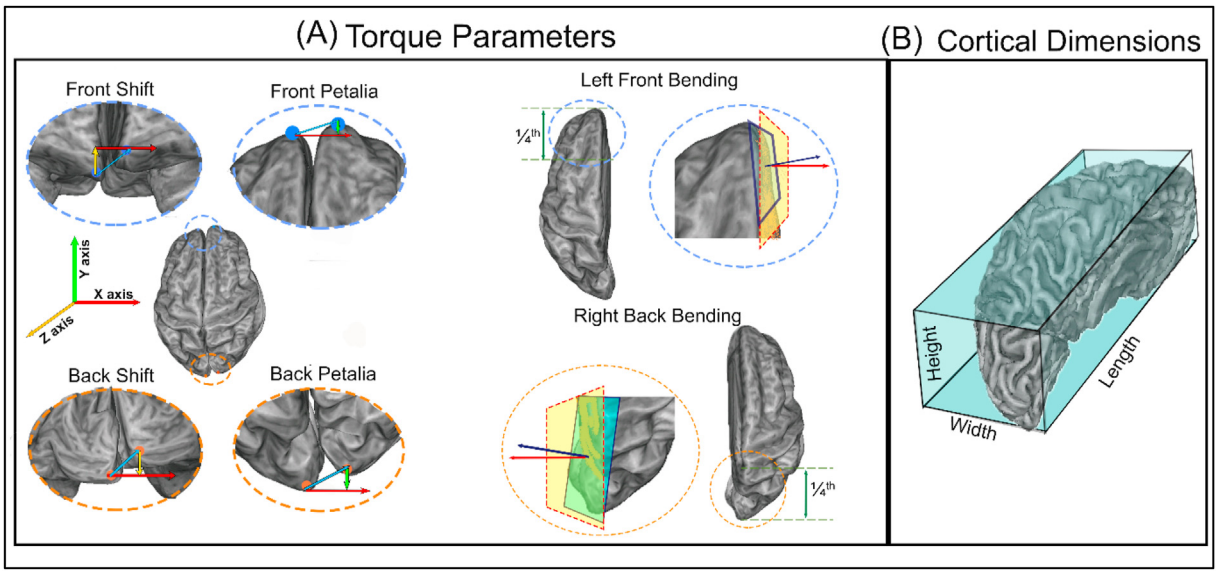

Fig. 1. (a) Brain torque computation illustration (for details, refer to Xiang et al., 2019). The front and back shifts are calculated as the distance between the two extreme points located within the two hemispheres' left and right frontal and occipital poles along the XZ plane, respectively. Similarly, the displacement of the left and right hemispheres along the XY plane at frontal and occipital poles were calculated as front and back petalias. The X, Y, and Z axes are represented in red, green, and yellow colors, whereas the displacement measurement is represented in blue color. The third column illustrates the calculation of bending angles. The blue plane represents the fitted least square plane to the vertices in the medial surface of the frontal and occipital quarters of the brain. The yellow plane represents the midsagittal plane at x = 0. The bending is the angle between the surface normal to the fitted plane (blue) and the surface normal to the midsagittal plane (red). (B) shows the measurement of cerebral dimensions as an enclosed parallelepiped to the cerebral hemisphere with its edges parallel to the MNI coordinates. (For interpretation of the references to color in this figure legend, the reader is referred to the Web version of this article.)

>27] met the hearing, vision, and English language ability criteria, free of MRI contraindications and neurologic or psychiatric conditions, were recruited for stage 2. This study was approved by the local ethics committee, Cambridgeshire 2, Research Ethics Committee (reference: 10/H0308/50).

During stage 2, all MRI images were collected using a 3T Siemens TIM Trio scanner with a 32-channel head coil. T1 weighted images were collected using MPRAGE sequence, TR = 2250 ms (ms), TE = 2.99 ms, flip angle = 9°, Voxel size = 1 × 1 × 1 mm^3, FOV = 256 × 240 × 192 mm^3, GRAPPA: 2; TI: 900 ms. All the selected images passed a quality control checked by a semi-automated script monitored by the CAM-CAN team. All right-handed individuals (based on the handedness scores) were selected and arbitrarily divided the data into three groups: young (group A: between >18 and ≤41 years), middle-aged (group B: between >41 and ≤64 years), and older age (group C: between >64 and ≤87 years). Each group had 80 MRIs (*Total n* = 3 *age groups* × 2 *sex* × 40 *images of each sex* = 240). Within each age group males and females didn't significantly differ ($p > 0.05$) in, height, weight, handedness, MMSE, anxiety, depression, and sleep quality scores, as shown in Table 2.

2.2. Data simulation

Each MRI image underwent the following analysis: (i) Simulation of tDCS current spread using ROAST, (ii) Estimation of current intensity at target ROI using i-SATA, (iii) Calculation of brain volumes CSF, GM, and WM using CAT12, and (iv) Calculation of cerebral dimensions and torque parameters using the methodology reported in Xiang et al., [37,38]. These steps are described in detail as follows.

2.2.1. Simulation of tDCS

Individual T1-weighted images were modelled using ROAST V3.0 [65]. Two electrode montages (based on the 10–20 EEG System), namely CP5_CZ (anode at CP5 and cathode at Cz) and F3_FP2 (anode at F3 and cathode at Fp2), were simulated. These two montages were selected for three reasons: (1) The parietal (CP5_CZ) and frontal (F3_FP2) locations were of particular interest as Russel et al. [69] reported sex differences in frontal and parietal bone density and also the resultant simulated tDCS current density. (2) Prior simulation studies have well established that the target regions, the left IPL and the left MFG, are optimally targeted by CP5_CZ [43]and F3_FP2 [44], respectively. (3) Finally, these two montages are used by most of the tDCS studies to modulate specific cognitive functions such as reading behaviour (CP5_CZ) [43] and depression (F3_FP2) [44]. These bipolar montages were modelled with electrode pads of size 5 × 5 cm^2 and 3 mm thickness. Rectangular bipolar electrodes were used because a prior study has shown that this electrode configuration produces the most homogenous field in the target ROI, compared to other electrode types [70]. Whilst 3 × 3 cm^2 and 5 × 7 cm^2 electrode pads also exist in the literature, prior evidence suggests a negligible change in pattern of distribution in current density with electrode sizes [43]. These montages were simulated with 2 mA current intensity. At this point, it is worth mentioning that a study has shown that at least 4–6 mA current is needed to produce reliable neuronal activity using animal models and human cadavers [71]. However, more investigations are required regarding the safety and tolerability of participants in using such high current intensities [72]. Hence we restrict our simulations only to 2 mA as commonly used maximum current intensity in tDCS studies to improve cognitive function with successful blinding [73]. The values of conductivities of various tissues (as inbuilt in ROAST) were utilised for white matter (0.126 S/m); grey matter (0.276 S/m); cerebrospinal fluid (1.65 S/m); bone (0.01 S/m); skin (0.465 S/m); air (2.5 e^{-14} S/m); gel (0.3 S/m); and electrode (5.9 e^7 S/m)). ROAST's outputs, which are the current density (mA/m^2) corresponding to each node (x, y, and z co-ordinates), were obtained. The ROAST output could also be in Electric field intensity (E), a frequently used parameter in the tDCS studies. Current density (J) is related to E as in J = σE, where J = current density (A/m^2), E = Electric field intensity (V/m) and

σ = resistivity of the tissue. J and E demonstrate equivalent distribution when resistivity in the cortex is maintained constant.

2.2.2. Estimation of current density at target ROIs

The output from the ROAST for each T1 image was post-processed using i-SATA. ROAST simulates each brain in the native space to provide two outputs as coordinate and magnitude of electric field (norm values) matrices. The i-SATA converts the coordinate matrix of each head (as supplied by ROAST) to Talairach space [for details, refer to, 56]. The converted coordinates are projected to the Talairach Client, and anatomical boundaries of the ROIs are demarcated according to the Talairach template (similar to [43,66]). The corresponding magnitudes of current density received by each lobe and gyrus are averaged. For the convenience of the readers, the top 10% of the regions with maximum average current density are shown in Figs. 2 and 3. Thus, the total current density at each target ROI: left IPL and left MFG (w-target) was also calculated for both the tDCS montages.

2.2.3. Estimation of volume parameters

Volume parameters for each T1 image were calculated using the CAT12 toolbox (version 12.7) [74]. The images were corrected for bias–field inhomogeneity and spatially normalized using the DARTEL algorithm. The scans were then segmented into GM, WM, and CSF volumes. The modulation of the segmented images was performed wherein tissue class images aligned with the template were multiplied with the Jacobian determinant derived from the spatial normalization [74,75]. This step ensures that the tissue volumes get corrected for individual differences in brain size [76]. The segmented images are then smoothed by convolving with an isotropic Gaussian kernel of 8-mm FWHM size [74]. After pre-processing, all the images passed the quality control in CAT12, and the weighted overall image quality index and mean correlation of our sample (n = 240) were 1.98 ± 0.03 and 0.91 ± 0.01, respectively. The absolute GM, WM, and CSF volumes were standardized with the respective total intracranial volume (TIV) and referred to as relative GM (VolRelGM), WM (VolRelWM) CSF (VolRelCSF) volumes.

2.2.4. Estimation of torque parameters and cortical dimensions

The coordinate matrix (or the vertices) of individual MRI (obtained from ROAST) were used to determine the length and torque parameters using the methodology described by Xiang et al. [37,38]. The matrix was divided into two hemispheres by selecting the midsagittal plane passing through anterior commissure, posterior commissure, and midsagittal points. The extreme points on each cerebral hemisphere along the anterior-posterior axis were demarcated as the frontal and occipital poles. Front and back shifts were the displacements of the left and right frontal and occipital poles along the XZ plane (Fig. 1A). Similarly, front and back petalias were the respective displacements of left and right frontal and occipital poles along the XY plane (Fig. 1A). Front and back bending were computed in three steps - (1) The vertices in the first and last quarters of the medial surface of each hemisphere were identified, (2) A least-square plane was fitted onto the vertices of each quarter, and the surface normal to the respective planes was calculated, and (3) front and back bending values for each hemisphere were calculated as the angle (θ) between the surface normal to the fitted individual planes and the surface normal to the midsagittal plane (Fig. 1A). The asymmetry in bending was calculated as the difference of bending angles between left and right hemispheric at frontal (LR front bending) and occipital poles (LR back bending).

The three dimensions of the brain (Fig. 1B) that were measured for each hemisphere are latero-medial width (x distance), anteroposterior length (y distance), and dorso-ventral height (Z distance). These were the dimensions of the smallest orthogonal parallelepiped that would enclose the outer surface of each cerebral hemisphere with edges parallel to the three axes of the MNI coordinate system (Fig. 1B). We computed the ratios.

length/width (left LW and right LW), and *length/height* (left LH and right LH) for left and right hemispheres.

2.3. Statistical analysis

Initially, all the parameters obtained from the individual images were checked for the normality distribution using Shapiro-Wilk's method. The overarching aim of the present study was to investigate the effect of age and sex (both main and interaction effects) on w-target and the underlying anatomical factors contributing towards it. To this aim, four statistical analyses were performed: (1) As a starting point, a single model was designed using stepwise linear regression that considered the contribution of all the 16 parameters (including demographics and anatomical characteristics, refer to Table 3); (2) subsequently, the whole dataset was categorized into six groups (2 sex × 3 age groups), and group-level differences in w-targets was analyzed; (3) next, mediation analysis with multiple mediators was applied to each age group to evaluate the contribution of all cortical anatomy factors in predicting the sex difference in w-target; and (4) finally, the sex difference for each cortical anatomical parameter was analyzed separately through independent two-tailed *t-tests* within each age group. The association of each anatomic parameter with w-target was also analyzed independently. Each analyses has been described in details as follows.

2.3.1. Analysis of individual parameters

For each montage, a single stepwise linear regression model (using the 'stepwiselm' function in matlab) was used to investigate

Table 2
The participant's details in three age groups.

Items	GROUP A		GROUP B		GROUP C	
	MALE	FEMALE	MALE	FEMALE	MALE	FEMALE
Age (yrs)	36.6 ± 8.4	34.9 ± 8.7	52.7 ± 18.6	53.07 ± 7.8	74.2 ± 7.6	74.08 ± 7.5
Height (cm)	170.9 ± 20.6	169.4 ± 15.1	170.6 ± 15.1	169.5 ± 15.1	169.5 ± 15.1	169.5 ± 15.1
Weight (kg)	73.86 ± 16.6	75.84 ± 16.6	75.7 ± 16.6	75.7 ± 16.6	73.7 ± 16.7	75.7 ± 16.6
Handedness	84.9 ± 34.1	83.5 ± 41.0	79.7 ± 44.1	80.6 ± 41.01	83.3 ± 44.4	82.8 ± 45.2
MMSE	28.91 ± 1.21	29.17 ± 1.18	29.1 ± 1.05	29.1 ± 1.02	28.5 ± 1.28	28.5 ± 1.29
HADS_anxiety	5.6 ± 3.4	5.8 ± 3.5	4.8 ± 2.9	4.5 ± 2.8	4.2 ± 3.2	4.2 ± 3.2
HADS_depression	2.7 ± 2.8	2.8 ± 2.9	2.9 ± 2.8	2.5 ± 2.7	3.2 ± 2.5	3.3 ± 2.6
Sleep_efficiency	84.02 ± 13.1	86.7 ± 13.7	86.3 ± 10.7	86.09 ± 10.7	80.8 ± 12.4	80.9 ± 12.5
PSQI	5.2 ± 3.5	5.4 ± 3.7	4.7 ± 3.05	4.6 ± 3.0	5.9 ± 3.8	5.9 ± 3.9

MMSE (Mini-Mental State Examination), HADS (Hospital Anxiety and Depression scale), PSQI (Pittsburgh Sleep Quality Index). None of the parameters are significantly different within age groups and between sexes.

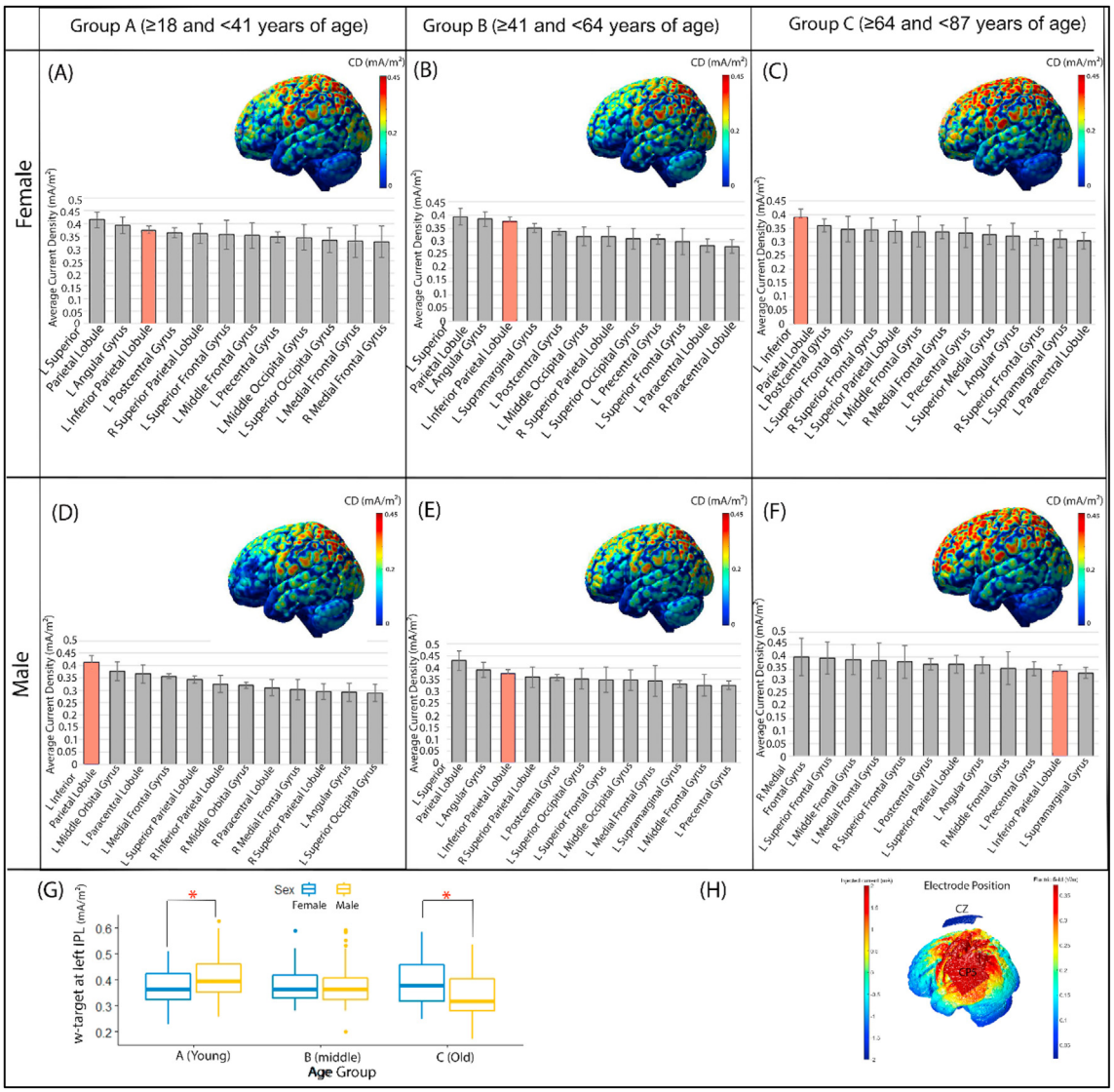

Fig. 2. A-F visualizes the spatial distribution of current density (CD) averaged across participants of the parietal montage CP5_CZ for males and females in young, middle-aged, and old-age groups (represented in three columns). The i-SATA outputs show the average CD (mA/m^2) in the top 10% of the brain regions, and the target region of interest, "Left inferior parietal lobule (left IPL)" is shown in pink color. (G) The difference in current at target region "Left inferior parietal lobule (left IPL)" (w-target, bar in pink color) between males and females across the three age groups. (H) Example of an electric field stimulation (ROAST output in v/m) with the electrode positions with anode at CP5, cathode at CZ with 5 × 5 cm^2 electrode sizes, and 2 mA of injected current. (For interpretation of the references to color in this figure legend, the reader is referred to the Web version of this article.)

the association of w-target with the 15 parameters (age, sex, 3 volume, 4 length, and 6 torque parameters). Backward elimination in stepwise regression allows the model to reduce parameters by selecting the most significant ($\alpha = 0.05$) variables. This procedure calculates the coefficient for each variable and level of significance (*p-value*). If the p-value is more than α, the variable is removed, and the linear regression is repeated with the remaining variables. When the *p-value* is less than α for all the variables, the process of backward elimination is complete. Moreover, when any item is linearly dependent with others in the current model, the 'stepwiselm' function removes the redundant term, regardless of the criterion value (*p-value*) (For additional analysis about checking of assumptions of the model, please refer to the supplementary)

2.3.2. Group-level differences in current density at target ROI

To determine how current intensity varied across the age groups and between sexes in each age group, we divided the results from the individual simulation into six groups. The i-SATA outputs from each T1 image, which provided a common reference head model, were averaged into six groups to visualize the mean current distribution across participants. Group-level analysis was performed using two separate ANOVA models with w-target as dependent variable and age (group A, B, and C) and sex as independent variables for both the tDCS montages.

2.3.3. Evaluating the contribution of anatomy parameters to sex difference

Mediation analyses with multiple mediators were performed for each age group using the 'mma' package developed in R software (for details, refer to Yu et al. [77]). We used mediation analysis to investigate the contribution of each cortical anatomic parameter (volume, dimension, and torque) to determine if there were differences in w-targets at two ROIs due to sex. Accordingly, sex was used as an independent variable, w-target as the dependent variable, and the rest of the volume, dimension, and torque parameters as mediators. Mediation analysis with multiple mediators allows

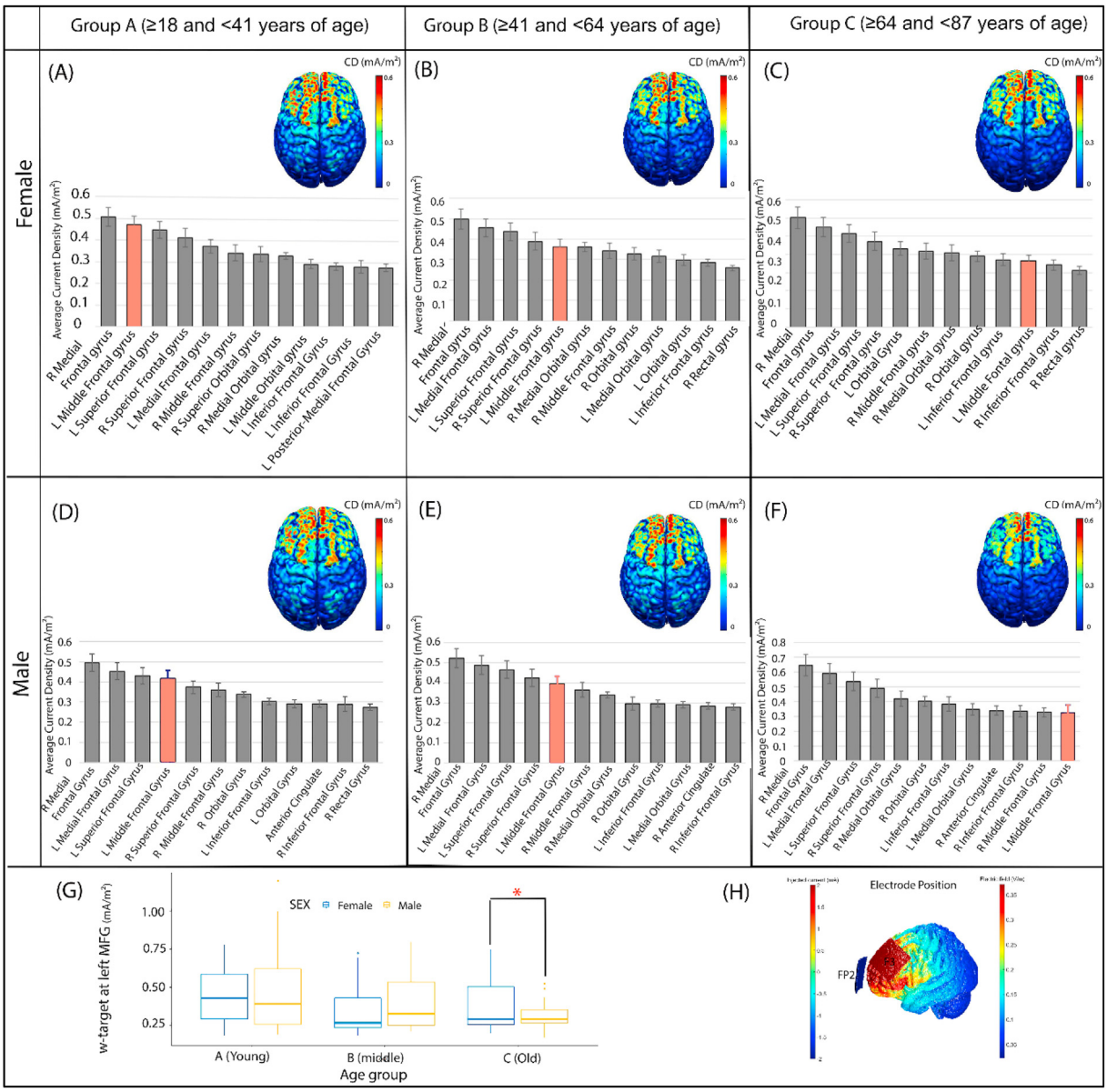

Fig. 3. A-F visualizes the spatial distribution of current density (CD) averaged across participants of frontal montage F3_FP2 for males and females in young, middle-aged, and old-age groups (represented in three columns). The i-SATA outputs show the average CD (mA/m^2) in the top 10% of the brain regions, and the target region of interest, " Left middle frontal gyrus (left MFG)" is shown in pink color. (G) The difference in current at target region "Left middle frontal gyrus (left MFG)" (w-target, bar in pink color) between males and females across the three age groups. (H) Example of an electric field stimulation (ROAST output in v/m) with electrode positions with anode at F3, cathode at FP2 with 5 × 5 cm^2 electrode sizes, and 2 mA of injected current. (For interpretation of the references to color in this figure legend, the reader is referred to the Web version of this article.)

estimation of individual effects of each parameter and joint-effects of multiple parameters. Bootstrap method with 5000 iterations was used to evaluate the significance of mediators as suggest by Preacher et al., [78].

2.3.4. Determining the sex difference in the cortical parameters and its association with current intensity at target ROI

A question that follows the mediation analysis is how the morphometric parameters change between males and females across the age groups? Although brain atrophy is expected with advancing age in both males and females, we calculated two measures evaluating the degree of cerebral atrophy:

$$\text{CSF/GM ratio} = \frac{VolRelCSF}{VolRelGM} \quad (1)$$

and

$$\text{Brain parenchyma fraction (BPF)} = \frac{absGM + absWM}{TIV} \quad (2)$$

The difference between males and females for these atrophy measures across the three age groups was analyzed using an independent two-tailed *t-test* with Bonferroni correction for multiple comparisons. Similarly, the sex difference between length and torque parameters was also calculated across the age groups. Additionally, the association of length and torque parameters with

Table 3
The fifteen parameters that are included in the analysis.

Demographics	Volumes	Length	Torque
Age	VolRelCSF $= \frac{\text{abs CSF}}{TIV}$	Left LW $= \frac{Left\ length}{left\ width}$	Front Shift
		Right LW $= \frac{Right\ length}{Right\ width}$	Back Shift
Sex	VolRelGM $= \frac{\text{abs GM}}{TIV}$	Left LH $= \frac{Left\ length}{left\ height}$	Front Petalia
		Right LH $= \frac{Right\ length}{Right\ height}$	Back Petalia
	VolRelWM $= \frac{\text{abs WM}}{TIV}$		LR(Left-Right) Front Bending LR (Left-Right) Back Bending

VolRelCSF = Relative volume of cerebrospinal fluid. VolRelGM = Relative volume of grey matter, VolRelWM = Relative volume of white matter, absCSF = absolute volume of cerebrospinal fluid, absGM = absolute volume of grey matter, absWM = absolute volume of white matter, TIV = Total intracranial volume.

atrophy measures was evaluated to determine whether any of the changes in these parameters are associated with cerebral atrophy. Finally, to determine how the change in atrophy influences the current intensity at target ROI, the association between atrophy measures and the w-target were analyzed for the three age groups (group A, B, and C), considering sex as a covariate.

3. Results

3.1. Analysis of the individual parameters

For the CP5_CZ montage targeting the IPL, we found a significant main effect of age ($p = 0.001$), sex ($p = 0.001$), VolRelCSF ($p = 0.005$), VolRelGM ($p = 0.01$), VolRelWM ($p = 0.004$), FrontShift ($p = 0.04$), FrontPetalias ($p = 0.04$), LeftLW ($p = 0.03$), RightLW ($p = 0.02$), LeftLH ($p = 0.001$). We also found a significant interaction of age and sex ($p = 0.04$) as shown in Fig. 4A.

For the F3_FP2 montage, we found significant main effects of age ($p = 0.001$), VolRelCSF ($p = 0.01$), VolRelGM ($p = 0.03$), VolRelWM ($p = 0.02$), FrontShift ($p = 0.008$), FrontPetalias ($p = -0.01$), LeftLH ($p = 0.005$), RightLH ($p = 0.004$). The main effect of sex and the interaction effect of age and sex was not significant ($p > 0.05$) for this montage. The predicted response of the age and sex interaction is shown in Fig. 5A.

3.2. Group-level differences in current density at target ROI

Fig. 2A–F and 3A-F show the group level averages of the total current intensity received by the top 12 brain regions (i-SATA output) for the parietal montage CP5_CZ and frontal montage F3_Fp2, respectively. The mean current intensity at the two ROIs of interest (w-targets), i.e., left IPL (for CP5_Cz) and left MFG (for F3_FP2), are highlighted in both figures. For the montage CP5_CZ following the two way ANOVA analysis (Fig. 2G), significant main-effect of age [$F(1, 2) = 3.43$, $p = 0.03$)] and interaction effect of age and sex [$F(1, 2) = 8.31$, $p = 0.0003$)] were found on w-target (IPL). Pair-wise comparison (Bonferroni corrected) revealed a decrease in current intensity in old age compared to the young age group ($p = 8.04e^{-}05$) and old age compared to the middle age group ($p = 0.012$) for males only. Males received higher current than females at the young age group ($p = 0.01$), whereas females received higher current than males in the old age group ($p = 0.004$) [Fig. 2G]. Similarly, for the montage F3_Fp2, a significant main effect of age [$F(1, 2) = 9.09$, $p = 0.0001$)] was found on the w-target for left MFG. Pair-wise comparison (Bonferroni corrected) reveals a decrease in current intensity in old age compared to the young age group for both males ($p = 0.0009$) and females ($p = 0.02$) and a decrease in middle age compared to young age group only for females ($p = 0.004$). Males had lower current intensity compared to females in old age group only ($p = 0.02$) [Fig. 3G].

3.3. Evaluating the contribution of anatomy parameters to sex difference

For the CP5_CZ montage (Fig. 4B, C and D), we found a significant total effect of sex in current density at IPL for both young (0.23, $p = 0.03$) and old age (0.34, $p = 0.04$) groups. In the middle age group, the total effect of (0.01, $p = 0.98$) of sex was negligible. Amongst the mediating factors, the indirect effects of VolRelCSF and VolRelGM made the highest contributions in determining the w-target at left IPL, irrespective of age group. In young age (Fig. 4A), VolRelGM (0.67, $p = 0.04$) has positive indirect effects whereas negative indirect effects of VolRelCSF (-0.857, $p = 0.06$) trended towards significance on the w-target at left IPL. Besides having a mediation effect, sex had a significant direct effect (0.13, $p = 0.04$), which means there was a significant effect of sex in the current density, even in the absence of the mediators considered in the analysis. In middle age, only the indirect effect of VolRelGM (1.01, $p = 0.04$) was significant. In the older age group, a positive indirect effect of VolRelCSF (0.93, $p = 0.04$) but negative indirect effect of VoRelGM (-0.81, $p = 0.05$) with current density was observed. These findings imply that the larger the CSF volume, the higher the current intensity at target ROI in old age, which is in contrast to young age, where larger is GM volumes, higher is the current intensity. In the older age group we found a joint effect of torque (0.2, $p = 0.02$) also to make significant contributions in determining the sex difference in current intensity (Fig. 4D).

For the F3_FP2 montage (Fig. 5B, C and D), the sex difference in current density at the left MFG was not seen for either young or middle-aged groups. A sex difference was seen only in older adults ($TE = -0.24$, $p = 0.04$). In middle age, VolRelCSF (1.12, $p = 0.03$) have a positive indirect effect and VolRelGM (-0.93, $p = 0.02$) have a negative indirect effects on w-target at left MFG. Similar association is also seen in old age with significant positive indirect effect of VolRelCSF (0.55, $p = 0.04$) and negative indirect effect of VolRelGM (-0.57, $p = 0.03$). In the old age group only, a joint indirect effect of brain-torque (0.27, $p = 0.04$) had a significant contribution to the sex difference in w-target.

3.4. Determining the sex difference in the cortical parameters and its association with current intensity at target ROI

Fig. 6A show that CSF/GM ratio increases as the age advances from young to old age for both the sexes. This suggests degree of brain atrophy increases with advancing age as confirmed by BPF values in Fig. 6B. It can be seen that BPF values are highest in young age (0.83 ± 0.03) and gradually declines through middle age

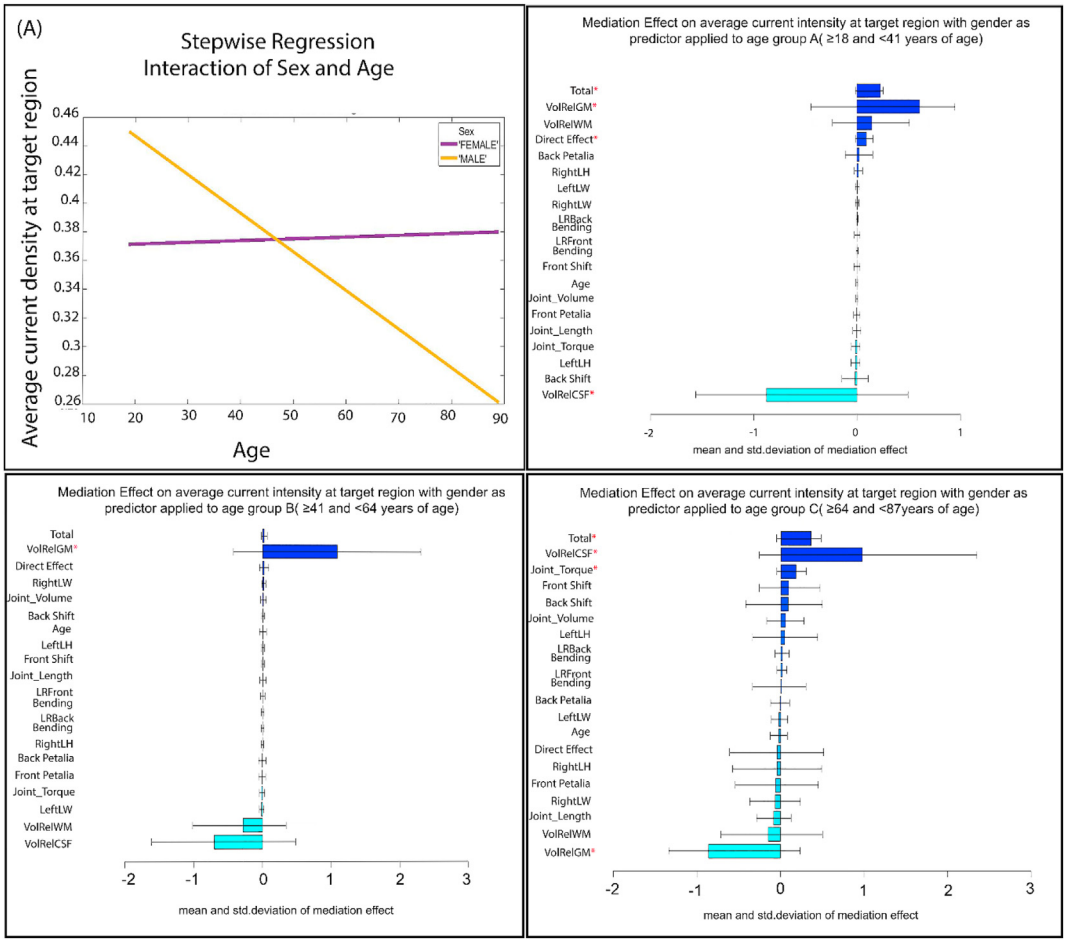

Fig. 4. (A) The interaction effect of age and sex at the targeted inferior parietal lobule ROI for the CP5_CZ montage. (B) The mediation analysis for the young age group shows a total effect and direct effects of sex and indirect effects of CSF and GM relative volumes. (C) In the middle age group, no significant total/direct effect of sex was seen but a significant indirect effects of VolRelGM was seen (D) in older adults, sex had a total effect on current intensity mediated by significant CSF and GM volumes and joint effect of brain-torque. The significant mediators are also marked with (*) in (B), (C) and (D).

(0.77 ± 0.02) and lowest in old age (0.68 ± 0.02). High BPF values and lower CSF/GM ratio at young age correspond with the positive indirect effect of VolRelGM to determine the current density at target ROI (as mentioned above in the mediation analyses). Similarly, Low BPF and high CSF/GM ratiovalues in old age correspond with the positive indirect effect of VolRelCSF on current density at target ROI. Fig. 6A also show that CSF/GM ratios is higher in females than males in all the three age groups but the difference widens as the age advances ($p < 0.1 \times 10^{-05}$). This sex difference in brain atrophy is confirmed by the brain parenchyma fraction (BPF) in Fig. 6B, where the gap between males and females widens in old age ($p = 0.14 \times 10^{-12}$) compared to the middle ($p = 0.259 \times 10^{-07}$) and young age ($p = 0.001$).

Additionally, males had a higher torque parameter (FrontShift) value compared to females ($p = 0.005$), as shown in Fig. 6C, which is driven by old agers (p = 0.34 × 10−06) only, but not by middle ($p = 0.29$) or young ($p = 0.33$) agers. Overall, males had a higher length by width ratio ($p = 0.004$) than females, mainly driven by males at a young age ($p = 0.01$, *figure not shown*). No significant sex difference was seen for length by height ratios in any of the age groups. To analyse whether the lower torque parameter in old females compared to males is associated with higher cerebral atrophy, regression of front shift with CSF/GM ratio and sex as independent factors was performed. We found a significant main effect of CSF/GM ratio (est = −7.83, $p = 0.007$), and sex (est = −7.49, $p = 0.008$) and interaction effect of CSF/GM and sex (est = 19.30, $p = 0.002$), as shown in Fig. 6D.

Subsequently, the association of the CSF/GM ratio with the w-target was analyzed using linear regression for age groups A, B, and C by considering sex as a covariate. The main effect of CSF/GM (est = −0.44, $p = 0.01$) was significant for group A, suggesting that the lower the CSF/GM ratio is associated with the higher the w-target values. Since males had a lower CSF/GM ratio than females, a higher w-target was seen for males than females, and a significant covariate factor of sex (est = −0.71, $p = 0.005$) was found. The main effect of CSF/GM was not found significant for groups B and C, but sex was found as a significant covariate for group C only (est = 0.11, $p = 0.007$). To this, when w-target was regressed with CSF/GM ratio separately for males and females in Group C, an opposite trend was seen (Fig. 6F). For males, higher CSF/GM ratio was associated with lower w-target (est = −0.73, $R^2 = 0.08$, $p = 0.02$). Whereas for females, higher the CSF/GM ratio was associated with higher w-

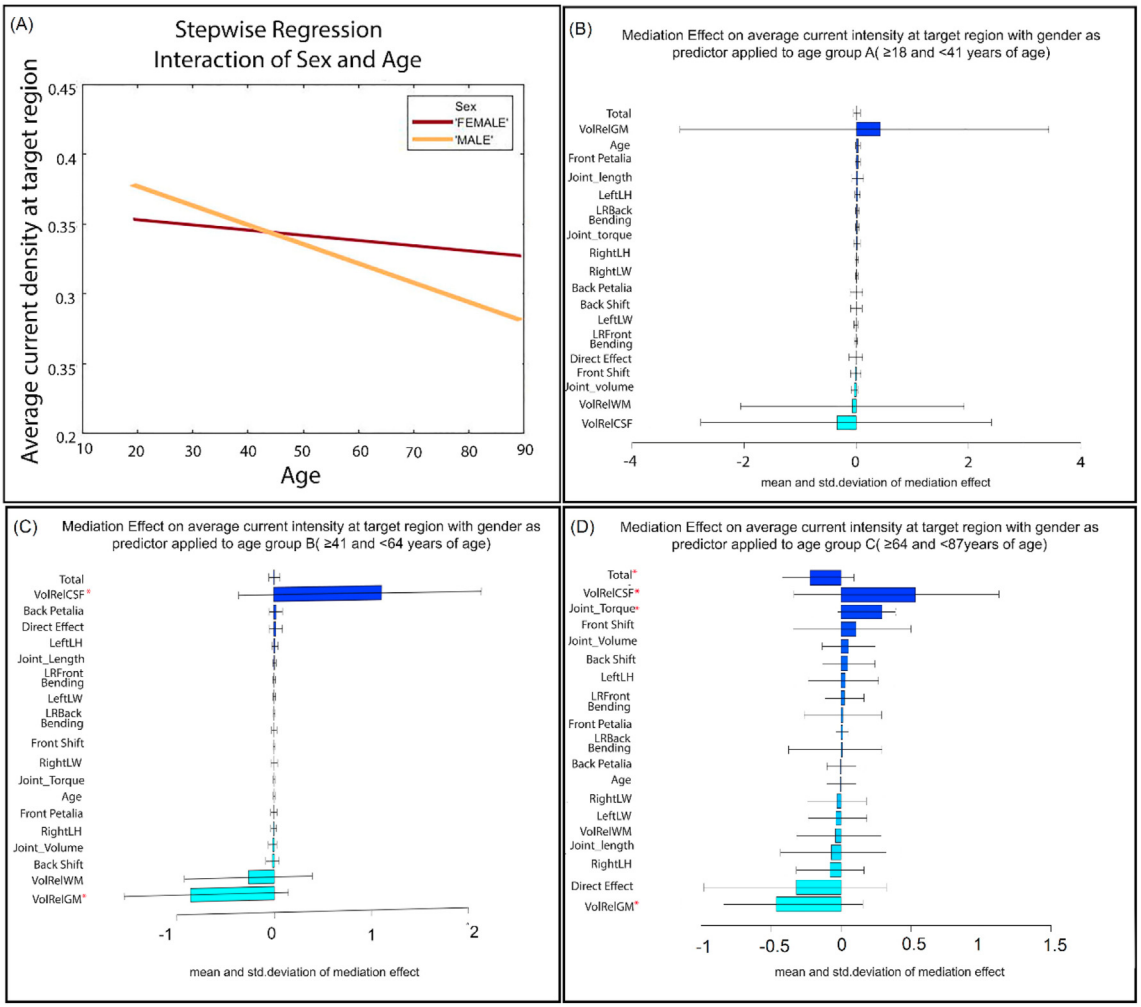

Fig. 5. (A) The interaction effect of age and sex at the targeted dorsolateral prefrontal cortex ROI for the F3_Fp2 montage. (B) The mediation analysis for the young age group showed no total effect or indirect effects (C). The mediation analysis in middle age show no significant total or direct effect of sex but shows the significant indirect effect of CSF and GM volumes (D) In older adults, sex had a total effect on current intensity mediated by indirect effects of CSF, GM volumes and joint effect of brain torque. The mediators are also marked with (*) in (B), (C) and (D).

target values (est = 0.38, R^2 = 0.05, $p = 0.04$). For all the above analyses, the normality and homogeneity of variance assumptions were not violated as tested by Shapiro-Wilk test and Barlett's test, respectively ($p > 0.05$).

4. Discussion

To the best of our knowledge, the present study is the first to simulate a large sample of individual MRIs for males and females across young to old age groups and investigate the association of current density at target ROI with15 cortical morphometric features. Such an analysis is expected to benefit future tDCS studies in tuning the tDCS stimulation parameters according to age and sex of an individual, so that response variability in tDCS could be minimized. Our analysis has four key findings- (i) Depending on age, the current density at targeted ROIs differed between males and females, (ii) CSF, and GM volumes played a significant role in determining the current density across all ages, (iii) sex difference across age groups in current density at a targeted site varies depending on the brain region stimulated (investigated through simulating frontal and parietal brain regions), and finally, (iv) structural hemispheric asymmetry quantified by torque plays a crucial role in mediating the sex difference in current density in the older age group only.

Overall, the present study found that the simulated current density that decreases with advancing age (refer to section 3.2) is associated with the atrophy-induced increase in CSF volume. This finding is in concordance with prior studies that investigated the association of age-related brain atrophy and tDCS current distribution [79–81], but these studies were limited in the number of brain MRIs being simulated (maximum three images). However, to the best of our knowledge, the present study is the first to report sexual dimorphism in simulated current intensity at older ages supported by our large sample size. The present study found that older females receive higher simulated current at target ROIs than their counterparts (parietal and frontal montages). A larger sex difference in current density at old age is mediated by higher CSF volume and lower GM volumes (Figs. 4 and 5D). When the association of CSF/GM ratio with w-target was investigated, a contrasting pattern was seen for males and females. For males, a higher CSF/GM ratio was associated with lower w-target values, but for females, higher CSF/GM ratios were associated with increased w-target values. Such reversal of the expected inverse relationship of current intensity with CSF volume in females could be related to

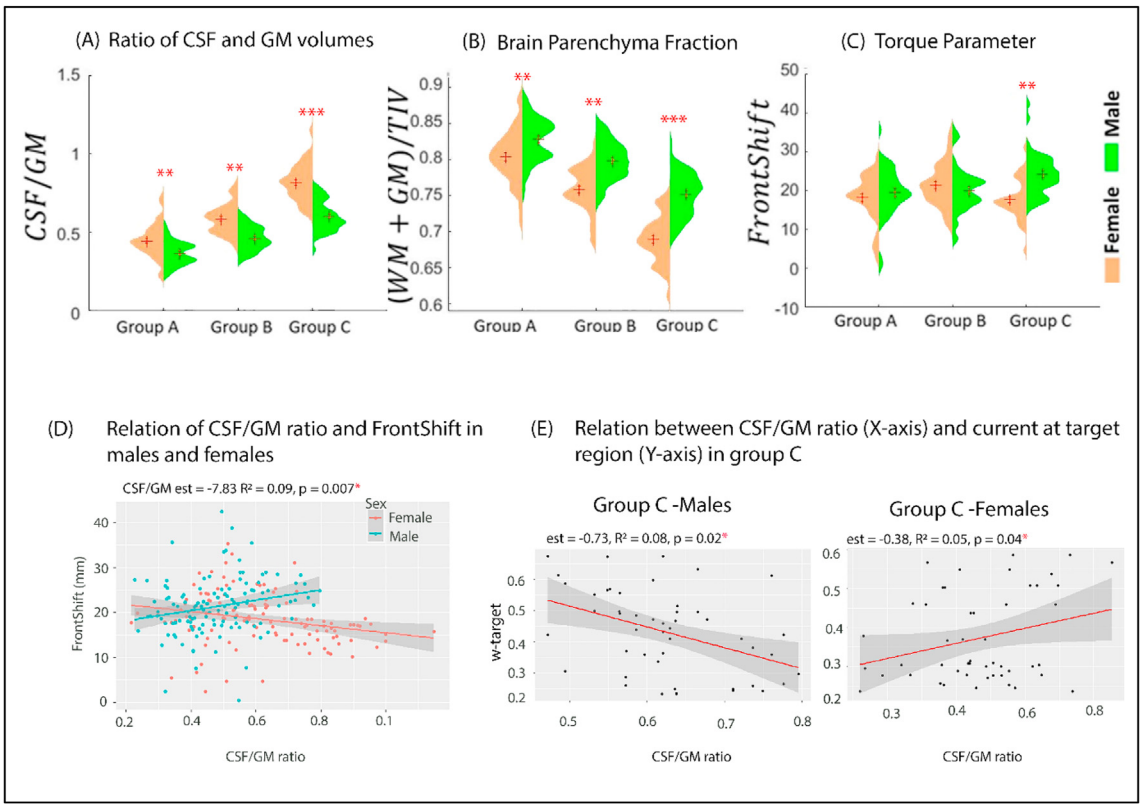

Fig. 6. Illustration of the parameters significantly different between males and females ($p < 0.001$) - (A) ratio of cerebrospinal fluid (CSF) to grey matter (GM) volume, (B) Brain parenchyma fraction (BPF), and (C) torque parameter (FrontShift) for three age groups (group A = ≥18 and <41 years, group B = ≥41 and <64 years, group C = ≥64 and <87 years of age). For CSF to GM ratio, and BPF, the values are significantly different between males and females for all the three age groups (denoted by *p < 10^{-03}, **p < 10^{-05}, ***p < 10^{-10}). In the case of FrontShift, significant sex difference was found only in old age (group C, denoted by **). The red (+) represents a mean and standard error, (D) The front shift in the y-axis is regressed with the CSF/GM ratio in the x-axis for males and females of the whole sample. (E) The relation between CSF/GM ration (x-axis) with current at target region (w-target in the y-axis) is shown for males and females of older age group only. (For interpretation of the references to color in this figure legend, the reader is referred to the Web version of this article.)

sex-related differences in brain aging. For example, prior studies have reported larger peripheral (sulcal) and lateral (Sylvian) fissure CSF volumes and apparent widening of sulcus in parieto-occipital regions for elderly males compared to females [82,83]. Specifically, Gur et al. [29] showed that the increase in the ratio of regional sulcal CSF to brain volume in males is significantly larger ($p < 0.0001$) than in females as their age progresses from young to old (refer to Fig. 3 in Gur et al. [29]). Since the conductivity of CSF is very high (1.71 S/m) compared to other tissue volumes like GM (0.47 S/m) and WM (0.22 S/m) [84], it is plausible that the greater regional (sulcal) accumulation of CSF volume in men might result in a preferential flow of current to the sulcal depths. Conversely, more current is left on the surface for females. Interestingly, such shunting of current injected to the brain (a phenomenon referred to as 'hot spots') due to brain atrophy has been reported previously in MCI and stroke patients [79–81].

Another factor contributing to such sex difference in current intensity at older ages (Figs. 4D and 5D) is the sex-specific dimorphism in the cerebral torque, which is reported for the first time in the present study. It was found that females have lower front shift values compared to males in older ages (Fig. 6C), but such difference is not seen in middle or young age. The observed sex difference in the torque parameters at older ages in the present study is associated with higher cerebral atrophy in females than males (Fig. 6E). It is interesting to note that cerebral atrophy has a complex interplay with other factors like cerebral torques to determine the current intensity in older ages. Altogether, our study reports the differential pattern of current distribution in old males and females and opens up new avenues for research that investigate the influence of regional sex differences in brain atrophy on tDCS current distribution.

In middle age, the sex difference in current intensity at target ROIs (both parietal and frontal) did not differ significantly between men and women. This finding is in concordance with a previous study investigating the variation in trajectories of the regional brain of healthy men and women aged from 20 to 85 years old, using longitudinal data collected from 122 adults (55 men and 67 women) with an interval of 8 years [83]. They reported an accelerated increase in CSF volumes of lateral ventricle, third ventricle, and Sylvian fissures in men compared to women only after 60 years of age. An exponential decrease in GM volumes was seen for both frontal and parietal cortices only after 60 years of age, more so for men than women. However, these increases (CSF volumes) and decreases (GM volumes) in brain volumes exhibited a linear pattern before 60 years of age with no significant difference between males and females (refer to 2 in Pfefferbaum et al. [83]). Thus, if the brain volumes mediate the current density at middle age (as shown in Figs. 4 and 5B), it is expected that no sex difference in current density at target ROIs can be seen.

At a young age, differences in the current density received by males and females at targeted ROIs vary depending on the location of the stimulated region. We found that young males received higher current than young females for the CP5_CZ montage over the parietal cortex. Interestingly, we found a similar trend for the

F3_FP2 montage, located over the frontal cortex, but the sex difference did not reach statistical significance. When the association of the CSF/GM ratio with w-target was investigated, a lower CSF/GM ratio was associated with higher current density at target ROI. Young males in the present sample have a lower global CSF/GM ratio than females, possibly due to their larger brain dimensions (refer to Fig. 6B); and hence males are expected to receive a higher current at target ROI. However, comparing regional volumes of left IPL and left MFG ROIs can facilitate our understanding of regional sex differences in current intensity between the two montages. In this aspect, prior studies investigating sex differences in regional CSF volumes are scanty, which seems to be the primary determinant for current distribution due to its highest conductivity. However, a sex difference in GM volumes was investigated from childhood to adulthood in a prior cross-sectional study of structural MRI data from 442 typically developing individuals (age range 8–30 years) [85]. In concordance with the present findings, their investigation revealed that lobar GM volumes (both parietal and frontal) are larger for males compared to females [85]. Interestingly, when the interaction effect of age and sex ($age^2 \times sex$) was investigated, they found the parietal lobe only survived correction for multiple comparisons of significance ($p < 0.001$) but the frontal lobe didn't [85]. These findings suggest the existence of a possible sex difference in the trajectory of regional cortical development. We believe that it would be helpful to investigate this relation with tDCS current spread for various montages in future studies.

Another possible reason for the difference in parietal region current density between males and females (males > females) could be due to the differences in skull density between the sexes (females > males) [86]. The effect of such sex differences in regional skull density on simulated tDCS current was reported by Russell et al. [69] by measuring the thicknesses of the three layers of the scalp using a combination of T1, T2, and proton density imaging. They found males (12 males ranging from 34 to 68 years) had more porous bone (a thicker spongy layer) than females (12 females ranging from 21 to 75 years), and the difference was higher for the parietal than the frontal bone. As a result, a higher simulated tDCS current density was found for males compared to females (skull modelled as three-layers of compact and spongiform layers), and the difference was more significant at the C3 (near temporoparietal) region compared to F3 (frontal) [86]. The present study also found that males receive more current at parietal montage ROI than females when the skull was modelled as a single compartment. The porous nature of the male skull might have contributed to this finding as studies have reported that single layer approximation and three-layered skull modelling don't produce much difference in the final simulated current [86,87], although the opposite view also exists [88].

To summarize, the present study reiterates that the inter-individual variability in cortical anatomy greatly influences the tDCS current distribution, as shown in previous studies. Specifically, the age range that undergoes rapid changes like the developing and aging brains are susceptible to more significant variations in tDCS current spread. Interestingly, both these categories are the likely populations that benefit from the application of tDCS. This variation emphasizes the need to individualize the tDCS modelling for different population categories and customize the stimulation parameters accordingly. In this direction, Evan et al. [89] recently proposed that the observed variability amongst individuals at the target ROI could be shifted from inside to outside by varying the stimulation dose. The present findings suggest that a specific cohort might need higher doses while low quantities might be sufficient for others. A recent simulation study supports this notion and shows that higher doses like three mA result in better selectivity in stimulating the target ROI than the non-target region in older adults (more so in males). But, a lower dose (1–2 ma) is enough to obtain the desired selectivity in younger adults [90]. Interestingly, studies have also shown that higher doses up to 4 mA could be safely used [72] but less tolerable in females compared to males [91]. Such personalized protocols need to be validated for generalization across populations while contemplating the sex differences in the tolerability of higher doses.

5. Limitations and future directions

The results in the present study are based on modelling and whether they would translate into behavioural or neurophysiological response needs further validation with empirical data. In this regard, women's hormonal status might also play a vital role as prior studies have demonstrated enhanced tDCS induced neurophysiological effects during high estrogen status of the late follicular phase of the menstrual cycle [refer to Table 1, 61]. Additionally, measures of neurotransmitter levels critical in tDCS responses (e.g., Gamma aminobutyric acid [GABA] and glutamate) support hormonal influences on cortical excitability [92]. Modelling approaches could also be influenced by electrode properties (shape, size, and conductivities of different electrode materials) [70]. However, it is reported that bipolar rectangular electrodes with saline beneath the electrodes produce a homogenous electric field at target ROI [70] and balances inter-individual variability, focality, and current magnitude [93]. Limitations regarding the segmentation procedure applied in tDCS modelling studies have also been reported but could benefit from including T2w images in future studies [94]. The conductivities of the tissue layers are considered constant in modelling studies. Differences in age-related changes in skull conductivity have been reported due to calcifications [84], which could, in turn, vary between males and females [95]. Although CSF conductivity seems relatively stable across the age groups [96], data regarding tissue conductivities across different age groups are scanty. Last but not least, only the norm component of the electric field was included in the study without any consideration to the direction of the current flow. The previous research has reported a reduced effect of bipolar electrodes on electric field magnitude variation [86], and directionality might not be that important when large areas covering numerous cortical folds are stimulated. However, the current direction might be relevant to the cortex's anatomy when specific gyri or sulci are stimulated by a more focal, high-definition electrode configuration [97]. Overall, modelling studies are helpful and can serve as a starting point to identify induced electrical current behaviour in recent years. However, future studies with neuroimaging methods like PET, cerebral blood flow and electrophysiological techniques could complement the tDCS modelling studies to clarify the associated physiological changes (for details [98,99]).

Although the results in the present study are encouraging, conclusions need to be drawn with caution as further empirical studies are required to understand the effect of the biology of sex in tDCS current distribution. The study considered the influence of sex difference in cortical parameters on tDCS-induced current density at the whole-brain level. Naturally, the effect of sex difference in regional morphometric factors underlying the target ROIs (for example, regional-cortical volumes, CSF and cortical thicknesses, surface area, convolution, and sulcal depth [25]) in regulating the spread of current across the brain region becomes an essential point for investigation. In this aspect, the amount of cancellous bone in the skull [100] through which the current percolates to the brain also deserves special attention. We keep it to the future studies to extract all such parameters from a multimodal (MRI, CT scans, etc.) and large dataset. In the present study, we considered the volumes in a normalized brain and have corrected for head size,

a practice commonly followed in all the volumetric analyses. An alternative way would be to perform the analysis in the native space and corroborate the findings. While doing so, we also suggest increasing the number of subjects in each group so that division of each age group into smaller bins can be performed to identify a smaller age range that exhibits the most apparent sex difference [101]. Finally, the present study reports the importance of one of the global cerebral asymmetries (Yakovlevian torque) in determining tDCS current density. Local asymmetries like planum parietale, central sulcus depth, parasagittal callosal measures, and grey matter posterior to central sulcus [25] should also be considered when montages positioning these regions are simulated. Such an investigation will enhance our understanding of the inter-individual variation in tDCS effects.

6. Conclusions

To conclude, depending on a person's age, the tDCS-induced current density at targeted ROIs could differ between males and females, mediated by variations in cortical anatomy. The motive is to highlight an influence of individual morphological changes in developing and degenerating brains on tDCS simulated current. To obtain desired stimulation benefits, individual modelling is needed to account for variability in cortical morphometry and to tailor the stimulation parameters.

CRediT authorship contribution statement

Sagarika Bhattacharjee: conceived the idea, performed, Formal analysis, and took the lead in planning and writing the manuscript. **Rajan Kashyap:** contributed with statistical, Formal analysis, were a part of technical discussions and contributed to manuscript preparation. **Alicia M. Goodwill:** were a part of technical discussions and, contributed to manuscript preparation. **Beth Ann O'Brien:** were a part of technical discussions and contributed to manuscript preparation. **Brenda Rapp:** were a part of technical discussions and, contributed to manuscript preparation. **Kenichi Oishi:** were a part of technical discussions and contributed to manuscript preparation. **John E. Desmond:** were a part of technical discussions and contributed to manuscript preparation, provided the overall guidance for the work. **SH Annabel Chen:** were a part of technical discussions and contributed to manuscript preparation, Funding acquisition, for the study was arranged.

Declaration of competing interest

The authors do not have any conflict of interest.

Acknowledgment

The work was funded by the NTU-JHU grant from Nanyang Technological University, Singapore. JD received additional support from NIH/NICHD grant P50 HD103538. SB and RK also received support from DBT Ramalingaswami Re-entry fellowship (2021), under the Government of India.

Appendix A. Supplementary data

Supplementary data to this article can be found online at https://doi.org/10.1016/j.brs.2021.11.018.

References

[1] Ruffini G, Wendling F, Merlet I, Molaee-Ardekani B, Mekonnen A, Salvador R, et al. Transcranial current brain stimulation (tCS): models and technologies. IEEE Trans Neural Syst Rehabil Eng 2012;21:333–45.
[2] Fertonani A, Miniussi C. Transcranial electrical stimulation: what we know and do not know about mechanisms. Neuroscientist 2017;23:109–23.
[3] Stagg CJ, Nitsche MA. Physiological basis of transcranial direct current stimulation. Neuroscientist 2011;17:37–53.
[4] Baharlouei H, Saba MA, Yazdi MJS, Jaberzadeh S. The effect of transcranial direct current stimulation on balance in healthy young and older adults: a systematic review of the literature. Neurophysiol Clin 2020.
[5] Tremblay S, Lepage J-F, Latulipe-Loiselle A, Fregni F, Pascual-Leone A, Théoret H. The uncertain outcome of prefrontal tDCS. Brain Stimu. 2014;7:773–83.
[6] Wiethoff S, Hamada M, Rothwell JC. Variability in response to transcranial direct current stimulation of the motor cortex. Brain Stimu. 2014;7:468–75.
[7] Huang Y-Z, Lu M-K, Antal A, Classen J, Nitsche M, Ziemann U, et al. Plasticity induced by non-invasive transcranial brain stimulation: a position paper. Clin Neurophysiol 2017;128:2318–29.
[8] Mikkonen M, Laakso I, Sumiya M, Koyama S, Hirata A, Tanaka S. TMS motor thresholds correlate with TDCS electric field strengths in hand motor area. Front Neurosci 2018;12:426.
[9] Laakso I, Tanaka S, Koyama S, De Santis V, Hirata A. Inter-subject variability in electric fields of motor cortical tDCS. Brain Stimu. 2015;8:906–13.
[10] Kim J-H, Kim D-W, Chang WH, Kim Y-H, Kim K, Im C-H. Inconsistent outcomes of transcranial direct current stimulation may originate from anatomical differences among individuals: electric field simulation using individual MRI data. Neurosci Lett 2014;564:6–10. https://doi.org/10.1016/j.neulet.2014.01.054.
[11] Antonenko D, Grittner U, Saturnino G, Nierhaus T, Thielscher A, Flöel A. Inter-individual and age-dependent variability in simulated electric fields induced by conventional transcranial electrical stimulation. Neuroimage 2021;224:117413. https://doi.org/10.1016/j.neuroimage.2020.117413.
[12] Kim J-H, Kim D-W, Chang WH, Kim Y-H, Kim K, Im C-H. Inconsistent outcomes of transcranial direct current stimulation may originate from anatomical differences among individuals: electric field simulation using individual MRI data. Neurosci Lett 2014;564:6–10.
[13] Mosayebi-Samani M, Jamil A, Salvador R, Ruffini G, Haueisen J, Nitsche MA. The impact of individual electrical fields and anatomical factors on the neurophysiological outcomes of tDCS: a TMS-MEP and MRI study. Brain Stimu. 2021;14:316–26. https://doi.org/10.1016/j.brs.2021.01.016.
[14] Datta A. Inter-individual variation during transcranial direct current stimulation and normalization of dose using MRI-derived computational models. Front Psychiatr 2012;3:91.
[15] Huang Y, Liu AA, Lafon B, Friedman D, Dayan M, Wang X, et al. Measurements and models of electric fields in the in vivo human brain during transcranial electric stimulation. Elife 2017;6:e18834.
[16] Indahlastari A, Albizu A, O'Shea A, Forbes MA, Nissim NR, Kraft JN, et al. Modeling transcranial electrical stimulation in the aging brain. Brain Stimu. 2020;13:664–74.
[17] Thomas C, Datta A, Woods A. Effect of aging on cortical current flow due to transcranial direct current stimulation: considerations for safety. In: 2018 40th Annual International Conference of the IEEE Engineering in Medicine and biology Society (EMBC). IEEE; 2018. p. 3084–7.
[18] Rudroff T, Workman CD, Fietsam AC, Kamholz J. Response variability in transcranial direct current stimulation: why sex matters. Front Psychiatr 2020;11:585.
[19] Dedoncker J, Brunoni AR, Baeken C, Vanderhasselt M-A. A systematic review and meta-analysis of the effects of transcranial direct current stimulation (tDCS) over the dorsolateral prefrontal cortex in healthy and neuropsychiatric samples: influence of stimulation parameters. Brain Stimu. 2016;9:501–17.
[20] Cotelli M, Manenti R, Gobbi E, Enrici I, Rusich D, Ferrari C, et al. Theory of mind performance predicts tDCS-mediated effects on the medial prefrontal cortex: a pilot study to investigate the role of sex and age. Brain Sci 2020;10:257. https://doi.org/10.3390/brainsci10050257.
[21] Adenzato M, Brambilla M, Manenti R, De Lucia L, Trojano L, Garofalo S, et al. Gender differences in cognitive Theory of Mind revealed by transcranial direct current stimulation on medial prefrontal cortex. Sci Rep. 2017;7:1–9.
[22] Adenzato M, Manenti R, Gobbi E, Enrici I, Rusich D, Cotelli M. Aging, sex and cognitive Theory of Mind: a transcranial direct current stimulation study. Sci Rep. 2019;9:18064. https://doi.org/10.1038/s41598-019-54469-4.
[23] Thomas C, Ghodratitoostani I, Delbem ACB, Ali A, Datta A. Influence of gender-related differences in transcranial direct current stimulation: a Computational Study. In: 2019 41st Annual International Conference of the IEEE Engineering in Medicine and biology Society (EMBC); 2019. p. 5196–9. https://doi.org/10.1109/EMBC.2019.8856898.
[24] Cahill L. Why sex matters for neuroscience. Nat Rev. Neurosci. 2006;7:477–84.
[25] Luders E, Toga AW. Sex differences in brain anatomy. Prog Brain Res. 2010;186:2–12.
[26] Cosgrove KP, Mazure CM, Staley JK. Evolving knowledge of sex differences in brain structure, function, and chemistry. Biol Psychiatr. 2007;62:847–55.

[27] Blatter DD, Bigler ED, Gale SD, Johnson SC, Anderson CV, Burnett BM, et al. Quantitative volumetric analysis of brain MR: normative database spanning 5 decades of life. Am J. Neuroradiol. 1995;16:241–51.
[28] Good CD, Johnsrude I, Ashburner J, Henson RN, Friston KJ, Frackowiak RS. Cerebral asymmetry and the effects of sex and handedness on brain structure: a voxel-based morphometric analysis of 465 normal adult human brains. Neuroimage 2001;14:685–700.
[29] Gur RC, Turetsky BI, Matsui M, Yan M, Bilker W, Hughett P, et al. Sex differences in brain gray and white matter in healthy young adults: correlations with cognitive performance. J Neurosci. 1999;19:4065–72.
[30] Lüders E, Steinmetz H, Jäncke L. Brain size and grey matter volume in the healthy human brain. Neuroreport 2002;13:2371–4.
[31] Filipek PA, Richelme C, Kennedy DN, Caviness Jr VS. The young adult human brain: an MRI-based morphometric analysis. Cerebr Cortex 1994;4:344–60.
[32] Goldstein JM, Seidman LJ, Horton NJ, Makris N, Kennedy DN, Caviness Jr VS, et al. Normal sexual dimorphism of the adult human brain assessed by in vivo magnetic resonance imaging. Cerebr Cortex 2001;11:490–7.
[33] Passe TJ, Rajagopalan P, Tupler LA, Byrum CE, Macfall JR, Krishnan K. Age and sex effects on brain morphology. Prog Neuro Psychopharmacol Biol Psychiatr 1997.
[34] Nopoulos P, Flaum M, O'Leary D, Andreasen NC. Sexual dimorphism in the human brain: evaluation of tissue volume, tissue composition and surface anatomy using magnetic resonance imaging. Psychiatr Res. Neuroimaging 2000;98:1–13.
[35] Schlaepfer TE, Harris GJ, Tien AY, Peng L, Lee S, Pearlson GD. Structural differences in the cerebral cortex of healthy female and male subjects: a magnetic resonance imaging study. Psychiatr Res. Neuroimaging 1995;61:129–35.
[36] Crivello F, Tzourio-Mazoyer N, Tzourio C, Mazoyer B. Longitudinal assessment of global and regional rate of grey matter atrophy in 1,172 healthy older adults: modulation by sex and age. PLOS ONE 2014;9:e114478. https://doi.org/10.1371/journal.pone.0114478.
[37] Xiang L, Crow T, Roberts N. Cerebral torque is human specific and unrelated to brain size. Brain Struct Funct. 2019;224:1141–50.
[38] Li X, Crow TJ, Hopkins WD, Gong Q, Roberts N. Human torque is not present in chimpanzee brain. Neuroimage 2018;165:285–93.
[39] Rentería ME. Cerebral asymmetry: a quantitative, multifactorial, and plastic brain phenotype. Twin Res Hum. Genet. 2012;15:401–13. https://doi.org/10.1017/thg.2012.13.
[40] Zilles K, Dabringhaus A, Geyer S, Amunts K, Qü M, Schleicher A, et al. Structural asymmetries in the human forebrain and the forebrain of non-human primates and rats. Neurosci Biobehav. Rev. 1996;20:593–605.
[41] Bear D, Schiff D, Saver J, Greenberg M, Freeman R. Quantitative analysis of cerebral asymmetries: fronto-occipital correlation, sexual dimorphism and association with handedness. Arch Neurol. 1986;43:598–603.
[42] Yang C, Zhong S, Zhou X, Wei L, Wang L, Nie S. The abnormality of topological asymmetry between hemispheric brain white matter networks in Alzheimer's disease and mild cognitive impairment. Front Aging. Neurosci. 2017;9:261.
[43] Bhattacharjee S, Kashyap R, Rapp B, Oishi K, Desmond JE, Chen SA. Simulation analyses of tDcS montages for the investigation of dorsal and ventral pathways. Sci Rep. 2019;9:1–17.
[44] Bai S, Dokos S, Ho K-A, Loo C. A computational modelling study of transcranial direct current stimulation montages used in depression. Neuroimage 2014;87:332–44.
[45] Gallucci A, Riva P, Romero Lauro LJ, Bushman BJ. Stimulating the ventrolateral prefrontal cortex (VLPFC) modulates frustration-induced aggression: a tDCS experiment. Brain Stimu. 2020;13:302–9. https://doi.org/10.1016/j.brs.2019.10.015.
[46] Yang X, Lin Y, Gao M, Jin X. Effect of modulating activity of dlpfc and gender on search behavior: a tDCS experiment. Front Hum Neurosci 2018;12. https://doi.org/10.3389/fnhum.2018.00325.
[47] Fumagalli M, Vergari M, Pasqualetti P, Marceglia S, Mameli F, Ferrucci R, et al. Brain switches utilitarian behavior: does gender make the difference? PLoS One 2010;5:e8865.
[48] Boggio PS, Rocha RR, da Silva MT, Fregni F. Differential modulatory effects of transcranial direct current stimulation on a facial expression go-no-go task in males and females. Neurosci Lett 2008;447:101–5. https://doi.org/10.1016/j.neulet.2008.10.009.
[49] Gao M, Yang X, Shi J, Lin Y, Chen S. Does gender make a difference in deception? The effect of transcranial direct current stimulation over dorsolateral prefrontal cortex. Front Psychol 2018;9. https://doi.org/10.3389/fpsyg.2018.01321.
[50] Ye H, Chen S, Huang D, Wang S, Jia Y, Luo J. Transcranial direct current stimulation over prefrontal cortex diminishes degree of risk aversion. Neurosci Lett 2015;598:18–22.
[51] León JJ, Sánchez-Kuhn A, Fernández-Martín P, Páez-Pérez MA, Thomas C, Datta A, et al. Transcranial direct current stimulation improves risky decision making in women but not in men: a sham-controlled study. Behav Brain Res. 2020;382:112485. https://doi.org/10.1016/j.bbr.2020.112485.
[52] Lapenta OM, Fregni F, Oberman LM, Boggio PS. Bilateral temporal cortex transcranial direct current stimulation worsens male performance in a multisensory integration task. Neurosci Lett 2012;527:105–9.
[53] Martin AK, Huang J, Hunold A, Meinzer M. Sex mediates the effects of high-definition transcranial direct current stimulation on "mind-reading. Neuroscience 2017;366:84–94. https://doi.org/10.1016/j.neuroscience.2017.10.005.
[54] Workman CD, Fietsam AC, Rudroff T. Transcranial direct current stimulation at 4 mA induces greater leg muscle fatigability in women compared to men. Brain Sci 2020;10:244.
[55] Frank E, Schecklmann M, Landgrebe M, Burger J, Kreuzer P, Poeppl TB, et al. Treatment of chronic tinnitus with repeated sessions of prefrontal transcranial direct current stimulation: outcomes from an open-label pilot study. J Neurol 2012;259:327–33. https://doi.org/10.1007/s00415-011-6189-4.
[56] Bertossi E, Peccenini L, Solmi A, Avenanti A, Ciaramelli E. Transcranial direct current stimulation of the medial prefrontal cortex dampens mind-wandering in men. Sci Rep. 2017;7:1–10.
[57] Wang S, Wang J, Guo W, Ye H, Lu X, Luo J, et al. Gender difference in gender bias: transcranial direct current stimulation reduces male's gender stereotypes. Front Hum Neurosci 2019;13. https://doi.org/10.3389/fnhum.2019.00403.
[58] De Tommaso M, Invitto S, Ricci K, Lucchese V, Delussi M, Quattromini P, et al. Effects of anodal TDCS stimulation of left parietal cortex on visual spatial attention tasks in men and women across menstrual cycle. Neurosci Lett 2014;574:21–5.
[59] Fehring DJ, Samandra R, Haque ZZ, Jaberzadeh S, Rosa M, Mansouri FA. Investigating the sex-dependent effects of prefrontal cortex stimulation on response execution and inhibition. Biol Sex Differ. 2021;12:47. https://doi.org/10.1186/s13293-021-00390-3.
[60] Bhattacharjee S, Kashyap R, O'Brien BA, McCloskey M, Oishi K, Desmond JE, et al. Reading proficiency influences the effects of transcranial direct current stimulation: evidence from selective modulation of dorsal and ventral pathways of reading in bilinguals. Brain Lang 2020;210:104850.
[61] Bhattacharjee S, Chew A, Kashyap R, Wu C, Yeo M, O'Brien B, et al. Could tDCS modulate bilingual reading? Brain Stimu.: Basic, Translational, and Clinical Research in Neuromodulation 2019;12:569. https://doi.org/10.1016/j.brs.2018.12.885.
[62] Kuo M-F, Paulus W, Nitsche MA. Sex differences in cortical neuroplasticity in humans. Neuroreport 2006;17:1703–7.
[63] Chaieb L, Antal A, Paulus W. Gender-specific modulation of short-term neuroplasticity in the visual cortex induced by transcranial direct current stimulation. Vis Neurosci. 2008;25:77–81. https://doi.org/10.1017/S0952523808080097.
[64] Lee S, Chung SW, Rogasch NC, Thomson CJ, Worsley RN, Kulkarni J, et al. The influence of endogenous estrogen on transcranial direct current stimulation: a preliminary study. Eur J. Neurosci. 2018;48:2001–12.
[65] Huang Y, Datta A, Bikson M, Parra LC. Realistic vOlumetric-Approach to Simulate Transcranial Electric Stimulation — ROAST — a fully automated open-source pipeline. BioRxiv 2018:217331. https://doi.org/10.1101/217331.
[66] Kashyap R, Bhattacharjee S, Arumugam R, Oishi K, Desmond JE, Chen SA, i-SATA. A MATLAB based toolbox to estimate current density generated by transcranial direct current stimulation in an individual brain. J Neural. Eng 2020;17:056034.
[67] Taylor JR, Williams N, Cusack R, Auer T, Shafto MA, Dixon M, et al. The Cambridge Centre for Ageing and Neuroscience (Cam-CAN) data repository: structural and functional MRI, MEG, and cognitive data from a cross-sectional adult lifespan sample. Neuroimage 2017;144:262–9.
[68] Shafto MA, Tyler LK, Dixon M, Taylor JR, Rowe JB, Cusack R, et al. The Cambridge Centre for Ageing and Neuroscience (Cam-CAN) study protocol: a cross-sectional, lifespan, multidisciplinary examination of healthy cognitive ageing. BMC Neurol 2014;14:1–25.
[69] Russell M, Goodman T, Wang Q, Groshong B, Lyeth BG. Gender differences in current received during transcranial electrical stimulation. Front Psychiatr 2014;5. https://doi.org/10.3389/fpsyt.2014.00104.
[70] Saturnino GB, Antunes A, Thielscher A. On the importance of electrode parameters for shaping electric field patterns generated by tDCS. Neuroimage 2015;120:25–35.
[71] Vöröslakos M, Takeuchi Y, Brinyiczki K, Zombori T, Oliva A, Fernández-Ruiz A, et al. Direct effects of transcranial electric stimulation on brain circuits in rats and humans. Nat Commun 2018;9:1–17.
[72] Workman CD, Kamholz J, Rudroff T. The tolerability and efficacy of 4 mA transcranial direct current stimulation on leg muscle fatigability. Brain Sci 2020;10:12.
[73] Fonteneau C, Mondino M, Arns M, Baeken C, Bikson M, Brunoni AR, et al. Sham tDCS: a hidden source of variability? Reflections for further blinded, controlled trials. Brain Stimu. 2019;12:668–73.
[74] Gaser C, Dahnke R. CAT-a computational anatomy toolbox for the analysis of structural MRI data. Hbm 2016;2016:336–48.
[75] Farokhian F, Beheshti I, Sone D, Matsuda H. Comparing CAT12 and VBM8 for detecting brain morphological abnormalities in temporal lobe epilepsy. Front Neurol. 2017;8:428. https://doi.org/10.3389/fneur.2017.00428.
[76] Cousijn J, Wiers RW, Ridderinkhof KR, van den Brink W, Veltman DJ, Goudriaan AE. Grey matter alterations associated with cannabis use: results of a VBM study in heavy cannabis users and healthy controls. Neuroimage 2012;59:3845–51.
[77] Yu Q, Li B. mma: an R package for mediation analysis with multiple mediators. J Open Res. Software 2017;5.

[78] Preacher KJ, Hayes AF. Asymptotic and resampling strategies for assessing and comparing indirect effects in multiple mediator models. Behav Res. Methods 2008;40:879–91.
[79] Minjoli S, Saturnino GB, JU Blicher, Stagg CJ, Siebner HR, Antunes A, et al. The impact of large structural brain changes in chronic stroke patients on the electric field caused by transcranial brain stimulation. Neuroimage: Clinical 2017;15:106–17.
[80] Unal G, Ficek B, Webster K, Shahabuddin S, Truong D, Hampstead B, et al. Impact of brain atrophy on tDCS and HD-tDCS current flow: a modeling study in three variants of primary progressive aphasia. Neurol Sci 2020;41: 1781–9. https://doi.org/10.1007/s10072-019-04229-z.
[81] Mahdavi S, Towhidkhah F, Initiative ADN. Computational human head models of tDCS: influence of brain atrophy on current density distribution. Brain Stimu. 2018;11:104–7.
[82] Coffey CE, Lucke JF, Saxton JA, Ratcliff G, Unitas LJ, Billig B, et al. Sex differences in brain aging: a quantitative magnetic resonance imaging study. Arch Neurol. 1998;55:169–79.
[83] Pfefferbaum A, Rohlfing T, Rosenbloom MJ, Chu W, Colrain IM, Sullivan EV. Variation in longitudinal trajectories of regional brain volumes of healthy men and women (ages 10 to 85 years) measured with atlas-based parcellation of MRI. Neuroimage 2013;65:176–93.
[84] McCann H, Pisano G, Beltrachini L. Variation in reported human head tissue electrical conductivity values. Brain Topogr 2019;32:825–58. https://doi.org/10.1007/s10548-019-00710-2.
[85] Koolschijn PCMP, Crone EA. Sex differences and structural brain maturation from childhood to early adulthood. Develop. Cognit. Neurosci. 2013;5: 106–18. https://doi.org/10.1016/j.dcn.2013.02.003.
[86] Rampersad S, Stegeman D, Oostendorp T. On handling the layered structure of the skull in transcranial direct current stimulation models. In: 2011 Annual International Conference of the IEEE Engineering in Medicine and biology Society. IEEE; 2011. p. 1989–92.
[87] Rampersad SM, Stegeman DF, Oostendorp TF. Single-layer skull approximations perform well in transcranial direct current stimulation modeling. IEEE Trans Neural Syst Rehabil Eng 2012;21:346–53.
[88] Sun W, Wang H, Zhang J, Yan T, Pei G. Multi-layer skull modeling and importance for tDCS simulation. Proceedings of the 2021 International Conference on Bioinformatics and Intelligent Computing. 2021. p. 250–6.
[89] Evans C, Bachmann C, Lee JS, Gregoriou E, Ward N, Bestmann S. Dose-controlled tDCS reduces electric field intensity variability at a cortical target site. Brain Stimu. 2020;13:125–36.
[90] Kashyap R, Bhattacharjee S, Arumugam R, Bharath RD, Udupa K, Oishi K, et al. Focality Oriented selection of current dose for transcranial direct current stimulation. 2021.
[91] Workman CD, Fietsam AC, Kamholz J, Rudroff T. Women report more severe sensations from 2 mA and 4 mA transcranial direct current stimulation than men. Eur J. Neurosci. 2021;53:2696–702. https://doi.org/10.1111/ejn.15070.
[92] Epperson CN, Haga K, Mason GF, Sellers E, Gueorguieva R, Zhang W, et al. Cortical γ-aminobutyric acid levels across the menstrual cycle in healthy women and those with premenstrual dysphoric disorder: a proton magnetic resonance spectroscopy study. Arch Gen. Psychiatr. 2002;59:851–8.
[93] Mikkonen M, Laakso I, Tanaka S, Hirata A. Cost of focality in TDCS: interindividual variability in electric fields. Brain Stimu. 2020;13:117–24.
[94] Puonti O, Saturnino GB, Madsen KH, Thielscher A. Value and limitations of intracranial recordings for validating electric field modeling for transcranial brain stimulation. Neuroimage 2020;208:116431. https://doi.org/10.1016/j.neuroimage.2019.116431.
[95] Schulte-Geers C, Obert M, Schilling RL, Harth S, Traupe H, Gizewski ER, et al. Age and gender-dependent bone density changes of the human skull disclosed by high-resolution flat-panel computed tomography. Int J. Leg. Med. 2011;125:417–25.
[96] Baumann SB, Wozny DR, Kelly SK, Meno FM. The electrical conductivity of human cerebrospinal fluid at body temperature. IEEE (Inst Electr Electron Eng) Trans. Biomed. Eng 1997;44:220–3.
[97] Dmochowski JP, Datta A, Bikson M, Su Y, Parra LC. Optimized multi-electrode stimulation increases focality and intensity at target. J Neural. Eng 2011;8: 046011. https://doi.org/10.1088/1741-2560/8/4/046011.
[98] Rudroff T, Workman CD, Fietsam AC, Ponto LLB. Imaging transcranial direct current stimulation (tDCS) with positron emission tomography (PET). Brain Sci. 2020;10:236.
[99] Kashyap R, Bhattacharjee S, Sommer W, Zhou C. Repetition priming effects for famous faces through dynamic causal modelling of latency-corrected event-related brain potentials. Eur J. Neurosci. 2019;49:1330–47.
[100] Russell M, Goodman T, Wang Q, Groshong B, Lyeth BG. Gender differences in current received during transcranial electrical stimulation. Front Psychiatr 2014;5:104.
[101] Rezaee Z, Dutta A. Lobule-specific dosage considerations for cerebellar transcranial direct current stimulation during healthy aging: a computational modeling study using age-specific magnetic resonance imaging templates. Neuromodulation 2020;23:341–65. https://doi.org/10.1111/ner.13098.